TORSIONAL-FLEXURAL BUCKLING OF THIN-WALL COLUMN OF OPEN SECTIONS

(USING RALEIGH-RITZ ENERGY METHOD)

BY

IKENNA M. NWACHUKWU (B.Eng, IMSU)

20174079248

A THESIS SUBMITTED TO THE POSTGRADUATE SCHOOL, FEDERAL UNIVERSITY OF TECHNOLOGY, OWERRI

IN PARTIAL FULFILLMENT OF THE REQIREMENTS FOR THE AWARD OF MASTER OF ENGINEERING (M. ENG.) DEGREE IN CIVIL ENGINEERING (STRUCTURAL ENGINEERING OPTION)

AUGUST, 2025

CERTIFICATION

This is to certify that this thesis, "Torsional-Flexural Buckling of Thin-Wall Column of Open Sections" carried out by Ikenna Nwachukwu, (B.Eng) with reg. No. 20174079248 and presented at postgraduate school, Federal University of Technology, Owerri, has been approved as meeting the requirements for the award of Master of Engineering.

Engr. Prof. D.O Onwuka — 09/09/2025
(Supervisor) — Date

Engr. Dr. F.C Njoku — 09/09/25
(Co-Supervisor) — Date

Engr. Dr. (Mrs.) J. I. Arimanwa — 24/09/2025
(Head of Department) — Date

Engr. Prof. Remy Uche — 06/10/25
(Dean of School of Engineering and Engineering Technology) — Date

Prof. Mrs. J.N. Nwosu — ---
(Dean of Postgraduate School) — Date

External examiner — ---
Date

DEDICATION

This Thesis is dedicated to Pastor Evelyn Joshua, whose unwavering commitment to serving God has been a beacon of hope and healing in our world today. Through her selfless dedication and steadfast faith, she has been instrumental in saving lives and demonstrating the power of divine strength.

ACKNOWLEDGEMENTS

I would like to express my deepest gratitude and appreciation to my esteemed supervisors, Engr. Prof. D.O Onwuka and Engr. Dr. F.C Njoku, for their invaluable guidance, unwavering support, and immense contributions throughout the course of my project.

My heartfelt appreciation and gratitude goes to Engr. Dr. O. M. Ibearugbulem for his valuable assistance and support throughout the course of my project.

I also wish to acknowledge my Head of Civil Engineering Department Engr. Dr. (Mrs.) J. I. Arimanwa, Dean, School of Engineering and Engineering Technology Engr. Prof. Remy Uche, Dean, School of Post Graduate Studies Prof. B. O. Esonu, Engr. Prof. J. C. Ezeh, Engr. Prof. (Mrs.) B. U. Dike, Rev. Engr. Prof. L. O. Ettu, Engr. Prof. J. C. Osuagwu, Engr. Dr. U. C. Anya, Engr. Dr. H. U. Nwoke and Engr. Prof. (Mrs.) C.E. Okere, Engr. Dr. Lewechi Anyaogu, Engr. Dr. C. I. Onyechere, Engr. A. N. Nwachukwu, Engr. A. P. C. Amanze, Engr. Kelechi Njoku, Engr. K. N. Onyema, Rev. Engr. Dr. N. L. Nwakwasi, Engr. Dr. O. R. Onosakponome, Engr. Anthony U. Igbojiaku, Mr C. A. Ajoku, Nnanna S. Ogbonna, Engr. Ihemegbulem Ezekiel, Engr. Mrs. P. N. Ikpa, Engr. Nwokorobia Godfrey Chimezie, Engr. Bertram Duke, Mr. C. S. Uzoukwu, Mrs. Jane Chidirim Maduagwu, and every other staff of the Civil Engineering Department for their encouragement.

Above all, I must give thanks to God Almighty, the fountain of wisdom and life. It is by His power and love that I was able to arrive at this. All praise, adoration and glory be to you now and forever.

LIST OF TABLES

LIST OF FIGURES

SYMBOLS AND NOTATIONS

Coordinates, Stress, Strains, Loads and Energy

ϕ	Angle of deformation
$d\phi$	angle of twist
P	Applied axial load
O	centroid
x, y, z	displacement direction
u, v, w	displacement field along x, y and z direction
ϕ	rotational displacement
v*, w*	displacement of the centroid along y-axis and z-axis
σ_x, σ_y, σ_z	Direct stress in directions x, y, z respectively
ε_x, ε_y, ε_z	Direct strain in directions x, y, z respectively
U_{xy}	flexural critical buckling load
$N_{cy}, N_{cz}, N_{c\omega}$	flexural critical buckling load for various second moments of area
τ_{xy}, τ_{xz}, τ_{yz}	Shear stress in planes xy, xz, yz respectively
γ_{xy}, γ_{xz}, γ_{yz}	Shear strain in planes xy, xz, yz respectively
τ_{xy}	Shear stress
γ_{xy}	Shear strain
I_z	second moment of area about (around) y axis
I_y	second moment of area about (around) z axis
S	shear centre
U	strain energy functional

J	St. Venant torsional constant
$\prod$	Total potential energy
V	Work done by external compressive load
I_ω	warping torsional constant

Section and material properties

A	Cross-section area
L	column length
O	centroid of section
C_y, C_z	Dimension
Y_0, Z_0	distance from O to B along Y and Z-axis
D	*Depth of section*
t_f	flange thickness
M	mass of cross section
B	shear center of the section
I	Second moment of area of cross-section
G	Shear modulus
t_w	Web thickness
B	width of section
E	Young's modulus

Table of Contents

ABSTRACT

This study focuses on determining the torsional-flexural critical buckling load of thin-walled columns with open cross-sections. An equation for torsional-flexural buckling analysis was formulated using the principles of the Ritz energy method. The analysis considers thin-walled columns with open cross-sections of arbitrary slope. During buckling, deformation is assumed to involve a combination of twisting and bending about the two principal axes of the cross-section. The total potential energy functional is assumed as the sum of the strain energy functional U and the potential energy due to the external compressive load V. The governing equations were found to reduce to an algebraic eigenvalue–eigenvector problem. Buckling equations were obtained for singly symmetric, doubly symmetric, and generally asymmetric column sections. The resulting buckling modes correspond to torsional-flexural buckling. Generally, the critical buckling loads decrease as the column length increases. The findings are in excellent agreement with Jerath (2020)'s solution. For thin-walled columns with doubly symmetric open cross-sections and hinged (simply supported) boundary conditions at x=0 and x=l, the governing differential equations, buckling modes, and buckling loads are uncoupled. The torsional-flexural buckling equations for thin-walled columns with open cross-sections result in a set of three uncoupled equations involving three displacement variables: u, v, and θ, representing translational and rotational displacements, respectively. In the case of thin-walled columns with singly symmetric open cross-sections under axial compressive loading through the centroid, the buckling behavior is governed by a set of three homogeneous differential equations, two of which are coupled.

Keywords: single symmetric columns, double symmetric columns, asymmetric column, flexural torsional buckling mode, algebraic eigen vector problem.

CHAPTER ONE

INTRODUCTION

1.1 Background Information

A thin-walled column is a structural member characterized by a slender geometry, where its length is significantly greater than its cross-sectional dimensions. These columns are especially valued for their ability to provide vertical support while minimizing material use and optimizing space. They are commonly employed in aerospace, automotive, marine, and civil engineering applications due to their high strength-to-weight ratio and structural efficiency.

Thin-walled structural elements are typically fabricated from isotropic materials such as steel and aluminum or from anisotropic and orthotropic materials like laminated composites. Common cross-sectional shapes include I, T, L, and C-shaped columns, which can be designed as either open or closed sections, and as singly or doubly symmetric profiles, depending on performance and application requirements.

One of the key advantages of thin-walled structures is their adaptability; they can be easily formed into various shapes with high shape factors, reducing material consumption while maintaining structural integrity. This flexibility, however, also introduces complexity. Thin-walled members are prone to various failure modes, including **local buckling, torsional buckling,** and **torsional-flexural buckling**, particularly under compressive loads. For example, composite plates within these members often exhibit local buckling before reaching their ultimate load-carrying capacity.

For different applications, thin-walled elements can be relatively easily formed into open or closed, singly or doubly symmetric cross-sections. They provide good strength and stiffness with a relatively

small amount of material. Designers have been taking the advantage of this weight efficiency in various applications where self-weight of the structure is a key design factor. Thin-wall columns are often employed in various architectural and structural applications, such as in high-rise buildings, bridges, and other structures where maximizing space efficiency is essential. These columns are typically made of materials with high strength-to-weight ratios, such as steel, reinforced concrete, or composite materials. The design of thin-wall columns involves considering their geometric properties, material properties, and the loads they will be subjected to. Several other factors are also important in their design, e.g the column's slenderness ratio (the ratio of its height to the least radius of gyration), the column's effective length, and the magnitude and type of applied loads (e.g., axial compression, bending, or a combination). Thin-wall columns are susceptible to buckling, which is the sudden lateral deflection or failure of the column under compressive loads. The buckling behavior depends on the column's slenderness ratio and boundary conditions. Proper analysis and design techniques, such as incorporating bracing or using

The **buckling behavior** of thin-walled members is a major design consideration. Due to their low torsional rigidity, members with open cross-sections are especially susceptible to **torsional-flexural buckling.** This is further complicated by the frequent misalignment of the centroid and shear center, which causes torsion and bending to interact, resulting in buckling at loads lower than the classical Euler critical load (Donnell, 1934).

Rozylo and Debski (2020) investigated Z-shaped composite thin-walled members, demonstrating improved structural performance through tailored cross-sectional design. Similarly, T-shaped thin-walled structures have been analyzed for use in aircraft rib applications, further highlighting the diversity of thin-walled component design in modern engineering.

The theoretical foundation for column buckling was laid by **Leonhard Euler** in 1744, who developed a model for a column fixed at one end and free at the other. In current engineering practice, however, the term "Euler column" commonly refers to a simply supported member, pinned at both ends (Jerath & Lee, 2015). Euler's classical analysis is based on several simplifying assumptions: the column is initially straight, the axial load is applied through the centroid, the material is homogeneous and follows Hooke's Law, and plane cross-sections remain plane during deformation.

While **static buckling theory** is effective for analyzing elastic instability under ideal conditions, it may be insufficient in real-world applications involving geometric imperfections, material nonlinearities, or complex boundary conditions. In such cases, more advanced numerical methods or experimental approaches are necessary to accurately predict behavior and ensure structural safety.

In open thin-walled sections, the structural response involve not torsion but also **distortional effects**. Distortion alters the geometry of the cross-section, generating additional stresses and potentially reducing the member's load-bearing capacity. Despite these challenges, the continued advancement of structural materials, design tools, and analytical techniques has significantly expanded the use of thin-walled structures in high-performance applications where **weight, efficiency, and space optimization** are critical design factors.

1.2 Problem Statement

Torsional-flexural buckling of thin-wall columns presents a significant challenge in the field of structural engineering. Despite advancements in design methodologies and material technologies, the complex behavior and failure mechanisms associated with thin-wall column buckling remain incompletely understood. This knowledge gap hampers engineers' ability to effectively predict and

prevent buckling failures in thin-wall column structures, thereby compromising their overall safety, stability, and structural performance. Additionally, the instability of the cross section further complicates the behavior of thin-walled structures.

While there have been notable strides in thin-walled structure research through experimental testing and theoretical investigations, there is still a need for further research as several important questions regarding torsional-flexural buckling remain partially answered or subject to controversy (Fang & Winter, 1965).

1.3 Aim and Objectives

The main of this study is to derive simplified stability equation for torsional-flexural (FT) buckling analysis of thin-walled columns of open sections. This research aims to achieve the following objectives:

i. To determine the total potential energy functional of a thin-walled column with open cross-section undergoing torsional-flexural buckling.
ii. To obtain the differential equation for the torsional-flexural buckling analysis of thin-walled columns with open cross-sections.
iii. To obtain elastic buckling equation using energy formulation for thin-walled columns with open cross-sections.
iv. To solve numerical problems with the method developed herein
v. To write a Visual Basic program to solve the problems of thin-walled columns with open cross-sections.

1.4 Justification of Study

The justifications of this study are;

1.4.1 **Improved Safety and Reliability**:

This study will help to enhance the safety and reliability of thin-wall column structures by developing a deeper understanding of the torsional-flexural buckling phenomenon. By unraveling the underlying failure mechanisms and accurately determining the load-carrying capacity, engineers can implement more effective design strategies and preventive measures to mitigate buckling failures. This research will contribute to minimizing the risk of premature column failure and ensure the structural integrity of thin-wall column structures.

1.4.2 **Advanced Design Guidelines**:

The study will also provide insights that will contribute to the development of advanced design guidelines for thin-wall column sections subjected to torsional-flexural buckling. By evaluating the impact of various factors, such as column geometry, material properties, loading conditions, and support conditions, the research will aid in formulating more accurate and reliable design recommendations. This will enable engineers to optimize the design of thin-wall columns, leading to more robust and efficient structures.

1.4.3 **Practical Implementation and Innovation**:

The research will bridge the gap between theoretical knowledge and practical implementation by considering the feasibility and compatibility of torsional-flexural buckling prevention strategies with existing design codes and industry standards. By addressing the practical aspects of implementation, the study aims to provide engineers with practical solutions and innovations that can be readily applied in real-world engineering projects. This will promote the safe and reliable utilization of thin-wall column structures while meeting the requirements of construction industry regulations.

1.4.4 **Advancement of Engineering Knowledge**:

Another justification of this study is contribution to the overall advancement of engineering knowledge in the field of torsional-flexural buckling of thin-wall columns. By conducting detailed investigations

and addressing key research questions, the study will fill the existing knowledge gaps and resolve controversies surrounding torsional buckling behavior. The findings will expand the understanding of the complex interaction between torsional and flexural modes of deformation, contributing to the broader body of knowledge in structural engineering.

1.5 Scope of Study

This study is limited to the analysis of buckling behavior in thin-walled structural members with open cross-sections, specifically focusing on torsional buckling, flexural buckling, and torsional-flexural buckling modes. It involves the determination of the total potential energy and the derivation of the differential equations governing the torsional-flexural buckling of thin-walled columns with open sections. The study also includes the evaluation of critical buckling equations for thin-walled columns with generally unsymmetrical, singly-symmetrical, and doubly-symmetrical open cross-sectional shapes. Additionally, a Visual Basic program was developed for the computation of the critical buckling loads, and the results obtained were validated to ensure accuracy and reliability. The scope is confined to thin-walled structures with open sections and does not extend to closed-section or thick-walled members.

CHAPTER TWO

LITERATURE REVIEW

2.1 Introduction

This section reviews some research works, their findings, and recommendation by several researchers concerning buckling, failure of compression members, torsional-flexural buckling etc. Hence these will be discussed below:

2.2 Thin-Walled Sections

In recent years, there has been a growing trend in the use of very slender thin-walled cross-sections members due to their high stiffness/weight ratio, as noted by Simao and Simoes da Silva (2004). Various industries, including civil, mechanical, naval, and aerospace, have been seeking stronger and lighter structural solutions to optimize effectiveness and cost, as highlighted by Andreassen (2012). As a result, thin-walled structures such as cold-formed steel beams and columns, steel and concrete box girders, ship hulls, trapezoidal steel sheeting, and other similar constructions have seen increased usage. These structures typically have one dimension significantly smaller than the others. They are commonly employed in civil, naval, space, offshore, and aerospace projects, serving as beams, columns, plates, shells, sheeting, pipes, and more.

2.2.1 Types of Thin-Walled Sections

From the stand point of torsional resistance, thin-Walled Sections (TWS) in general, are classified into three types (Nwachukwu, K. C., Ezeh, Ozioko, Eiroboyi, & Nwachukwu, D. C., 2021)

(a) Open Thin-Wall (OTW); in which a cell shear flow circuit cannot be established in the cross section. Examples are shown in Figure 2.1.

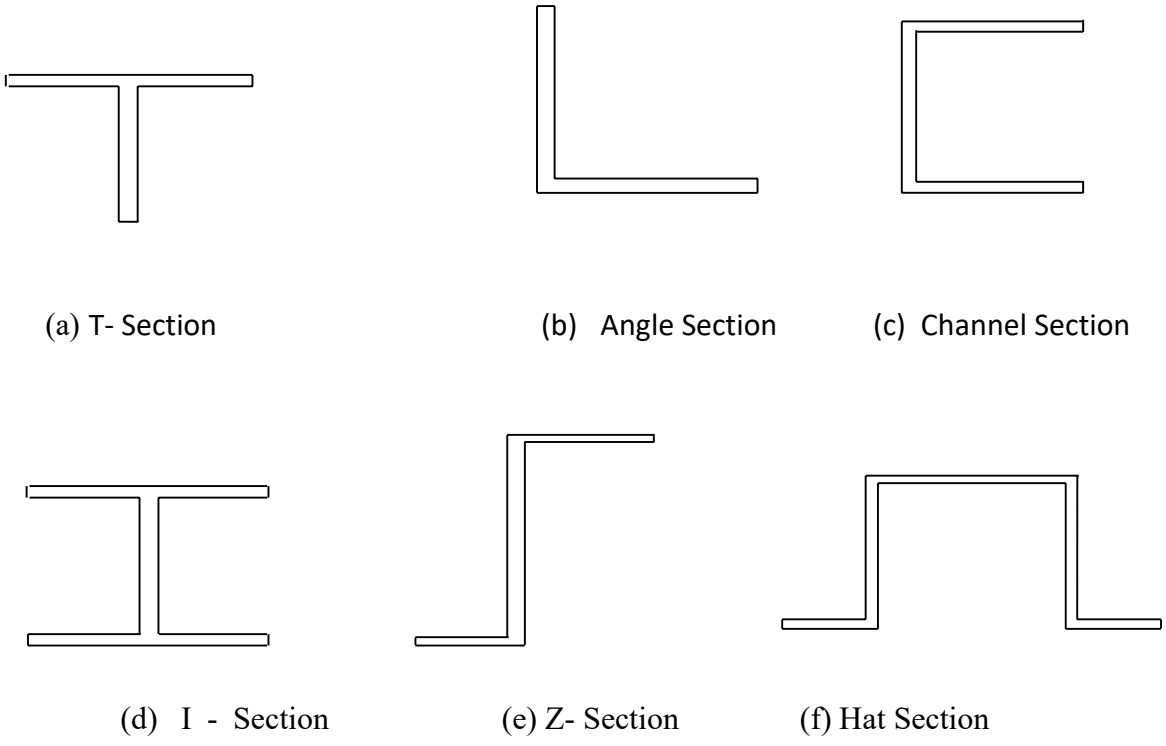

(a) T- Section (b) Angle Section (c) Channel Section

(d) I - Section (e) Z- Section (f) Hat Section

Figure 2.1: Examples of Thin-Walled Open Cross-Sections

(b) **Closed Thin- walled (CTW)**; in which at least one cell shear flow circuit can be established in the cross-section. Closed TW sections are in turn classified into single cell or multi-cell, according to whether one or several shear flow circuits, respectively can be identified. Examples of closed Thin-Walled sections are shown in Figure 2.2.

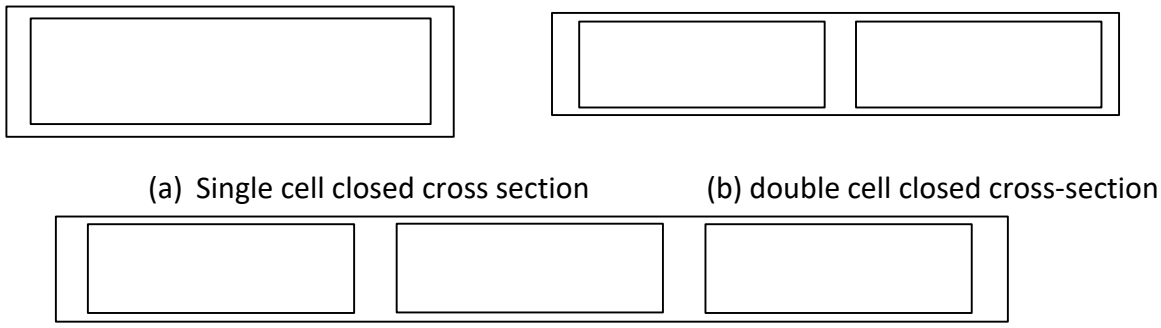

(a) Single cell closed cross section (b) double cell closed cross-section

(c) Triple cell closed cross-section

Figure 2.2: Examples of Thin- walled closed cross sections

(c) **Hybrid Thin- Walled (HTW)**: This type of section contains a mixture of Closed Thin-walled (CTW) and Open Thin-Walled (OTW) components. An example of HTW cross section is shown in Figure 2.3.

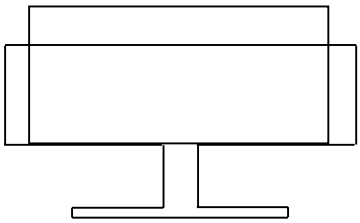

Figure 2.3: An example of Hybrid Thin- walled cross section

Thin-walled closed cross-section, especially the box typed structures can also have different types of arbitrary cross sections. Different types of arbitrary box cross- section are shown in Figure 2.4.

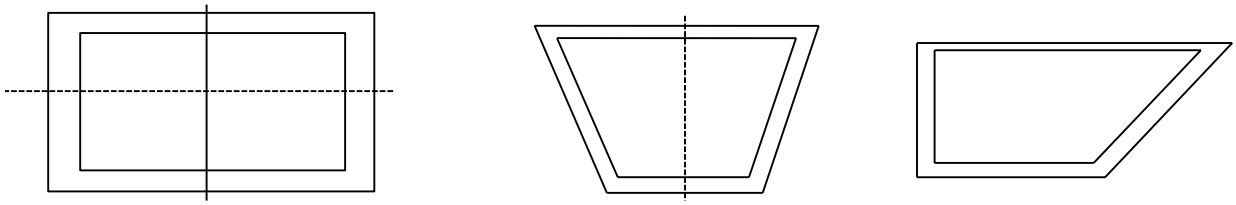

Doubly symmetric box section (b) Mono-symmetric box section (c) Asymmetric box section

Figure 2.4: Different Types of Arbitrary Box Cross-Section

2.3 Buckling

Buckling can be defined as the sudden large lateral deformation of structure due to a slight increase of axial compression load under which the structure had exhibited little, if any, deformation before the load was increased. If a structure is subjected to a gradually increasing load, when the load reaches a critical level, a member may suddenly change shape and the structure and component is said to have buckled Baird et al. (2011).

Buckling is a common phenomenon observed in thin-walled structures, referring to the loss of stability in a component due to lateral deflection when subjected to an axial force. The column's weakness causes it to bend, leading to rapid and potentially hazardous failure. Whether a column buckles depends on its length, strength, and other relevant factors. According to Baird et al. (2011), elastic buckling is more likely to occur in long columns relative to their thickness, or when an applied compressive load exceeds the critical allowable load of the thin-walled structure.

A standard thin-walled composite structure can be described in three major states: pre-buckling, critical buckling, and post-buckling. The loading process and carrying capacity of the structure are determined by buckling characteristics. The structure can still function even after buckling because the post-critical equilibrium trend is stable, and the increasing compressive load increases the wall deflection (Rozylo et al., 2020). Figure 2.5 below shows the state of each operation for a thin walled structure.

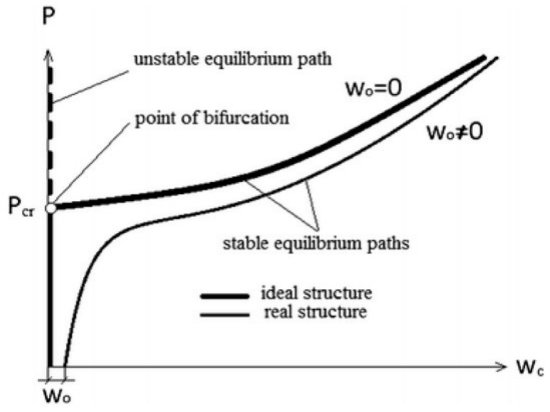

Figure 2.5 Graph of load applied versus deflection (Rozylo et al. 2020)

Where P, P_{cr} are the load and the critical buckling loads respectively. W_o, and W_c represent minimum and maximum deflection respectively. The point in the diagram where stability changes from stable to

unstable is called a bifurcation point. Buckling and carrying capacity determine the proper loading process of the structure.

Structural components might fail in different ways. Material properties such as yield stress often govern the failure mechanism of tension. For compression members, the failure mechanism is normally associated with instability issues where members suffer from some kind of buckling phe- nomenon. Various buckling phenomena associated with different structural components have been studied by a vast number of researchers in the past decades. The history of buckling theory dates back to the middle part of the 18th century, when Euler (1744) studied the buckling phenomenon of an incompressible, axially-loaded simply supported thin strut, or elastic. He described the mechanics of the strut using a mathematical technique that he had developed, known as 'the calculus of variations'; the governing differential equation for the strut for small deflections being expressed as:

$$EI\frac{d^4w}{dx^4} + P\frac{d^2w}{dx^2} = 0 \qquad 2.1$$

2.4 Buckling modes for Structural members

In general, the buckling failure usually occurs in thin-walled open cross-sections due to a combination of torsion and bending Jerath, (2020).The buckling mode represents the shape or pattern of the deformation that occurs during buckling. It is characterized by the bending or lateral deflection of the structure as it loses its ability to support the compressive load. Different structural elements can have various buckling modes, depending on their shape, boundary conditions, and material properties. When structural elements lack or have flexible intermediate restraints along their length, they are susceptible to buckling under compressive loads. From the work of (Wei-Wen, Roger, and Weiwen, 2010), closed sections typically do not experience torsional buckling due to their substantial torsional rigidity. Conversely, in

the case of open thin-walled sections, three potential modes of buckling are contemplated (Yu Wei-Wen, et al., 2010):

i. Flexural buckling
ii. Torsional buckling
iii. Torsional-flexural buckling

2.4.1 Flexural buckling

According to Yu Wei-Wen, et al., (2010), a slender axially loaded column may fail by overall flexural buckling if the cross section of the column is a doubly symmetric shape (I-section), closed shape (square or rectangular tube), closed cylindrical shape, or point-symmetric shape (Z-shape or cruciform). For singly symmetric shapes, flexural buckling is one of the possible failure modes,

Flexural buckling is easily identifiable as the most prominent mode of buckling for thin-walled structural members. When considering a pin-ended member that appears straight but possesses a minor imperfection causing it to deviate from perfect alignment, this deviation amplifies under axial compression. The critical point is reached, commonly for a steel member, when the combined axial and flexural stresses reach the yield stress at some section of the member. In the case of an I-section member that lacks restraint against transverse displacement, bending about the minor axis of the cross-section results in greater displacements and flexural stresses compared to bending about the major axis. Consequently, this member is said to buckle about its weak axis.

Flexural buckling in steel bridges is primarily a concern for trusses, where both chords and diagonals experience compression, as well as for bracing members subjected to compression.

In composite bridges, flexural buckling is typically a concern mainly for bracing members. However, in integral bridges, where the composite deck is subjected to a moderate axial force, flexural buckling is not the dominant mode of concern. Instead, the axial stresses and the interaction of buckling resistances become important factors that need to be considered when evaluating the buckling behavior of the bottom flange.

2.4.2 Torsional buckling

St Venant (1855) presented the first reliable work on the twisting response of structures. Doubly symmetric sections can experience torsional buckling, which involves twist only about their longitudinal axis. In cases like a cruciform section, the buckling load may be lower than that for flexural buckling, especially if the member is short.

Monosymmetric sections and asymmetric sections are susceptible to both torsional and flexural buckling modes, and sometimes these modes may occur at a lower load than flexural buckling about the minor axis. In bridges, these buckling modes are relevant primarily to angle and channel bracing members. Hendy and Murphy (2007) gave a comprehensive discussion on torsional modes.

2.4.3 Torsional-flexural Buckling

The earliest theoretical investigation of the torsional-flexural buckling problem was presented in Euler's 1759 work on column buckling, which gave the first analytical method to predict the reduced strengths of slender columns, and by Saint Venant's 1855 memoir on uniform torsion, which gave the first reliable description of twisting response of members to torsion (Trahair 1993). However, it was not until 1899 that the first published discussions of torsional-flexural buckling were made by Prandtl (1899) and Michell (1899), who considered the lateral buckling of beams with narrow rectangular cross-sections.

Subsequent work by Wagner (1929) and later work by Bleich (1952) and also by Timoshenko and Gere (1961) led to the development of a general theory of torsional-flexural buckling. They provided the classical energy equation for calculating the elastic flexural-torisonal buckling loads of thin-walled beams. Galambos (1963) introduced inelastic behavior of the torsional-flexural buckling; similar research was also presented by Lee (1960), White (1956), Wittrick (1952), and Horne (1950). All of these researches were done using the classical method, which provided exact solutions, yet it is limited by the necessity to make extensive calculations by hand. This situation changed dramatically with the advent of digital computers in the 1960's.

Researchers used numerical approaches that worked well with computers. There were many publications on various numerical approaches, such as Rayleigh Ritz method by (Wang, C. M., Wang, L., and Ang, K. K, 1994), the finite difference method by Bleich (1952), Assadi and Roeder (1985), and Chajes (1993), and the finite integral method by Trahair (1968), Anderson and Trahair (1972), and Kitipornchai and Trahair (1975). The finite element method was introduced by Barsoum and Gallagher (1970), in which they derived the stiffness equations for torsional-flexural instabilities of one-dimensional members with constant cross sections. During the later research, Powell and Klingner (1970) presented a lateral buckling analysis of an I-section beam, Hancock and Trahair (1978) considered the lateral buckling analysis of a monosymmetric cross-section beam with continuous restraints, Sallstrom (1996), Bradford and Ronagh (1997), and (Papangelis, Trahair, and Hancock, 1998). calculated the torsional-flexural buckling loads of beams, beam-columns, and plane frames, and Bazeos and Xykis (2002) presented research using the finite element method to analyze three dimensional trusses and frames.

More recent research on the theory of torsional-flexural buckling has been presented by Tong and Zhang (2003a) and (2003b) with their investigations of a new theory to clarify the inconsistencies of existing theories of the torsional-flexural buckling of thin-walled members. Ezeh (2010) investigated the

Behavior of Axially Compressed Multi-Cell Doubly Symmetric Thin-Walled Column using Vlasov's Theory.

Torkamani and Erin (2009) studied the elastic torsional-flexural buckling analysis of plane structures by considering second variation of the total potential energy of beam-column element and finite element method. Many of the developments of the torsional-flexural buckling theory have been made by extensions of the previously accepted theories, as expressed either by the differential equations of elastic bending and torsion or by energy equation for buckling. The classical energy equations for calculating the elastic torsional-flexural buckling load of thin-walled beams are usually assumed to be independent of the prebuckling deflections. Iyengar (1988) presented a work on torsional-flexural buckling of open section using equilibrium method. The torsional-flexural equations for column were derived for the hinged-hinged, clamped-clamped boundary conditions respectively. These equations were then used to obtain the critical buckling load for column sections with different ends conditions and buckling of unsymmetric section.

2.5 Experimental Studies

Since the 1960s, a large number of experimental investigations have also been conducted for cold-formed thin-walled steel columns with various types of cross-sections such as hat sections, channel sections, I-sections and box sections. Although the majority of the test data are associated with pure global buckling, some results highlighted the importance of the interaction between global and local buckling modes. In particular, Becque and Rasmussen (2009) approached an I-section column problem both experimentally and numerically for stainless steel specimens.

2.6 Formulas for Calculating Cross Section Properties

According to Canadian Institute of Steel Construction (CISC), Structural engineers occasionally need to determine the section properties of steel shapes not found in the current edition of the Handbook of Steel Construction (CISC 2000). Let us look at the formulas for calculating the torsional section properties of structural steel shapes of open sections. The section properties considered are the St. Venant torsional constant, J, the warping torsional constant, Cw.

2.6.1 Doubly-Symmetric Wide-Flange Shapes (W-Shapes and I-Beams)

In the determination of the formulas, the flange-to-web fillets are neglected. Galambos(1968) gave the formula for calculating the St. Venant torsional constant, J for an I-section. The torsional constant or torsion coefficient is a geometrical property of a bar's cross-section. It is involved in the relationship between angle of twist and applied torque along the axis of the bar, for a homogeneous linear elastic bar. More so, Galambos (1968), Picard and Beaulieu (1991) in their separate works determined the formula for calculating the warping torsional constant, I_{ω}.

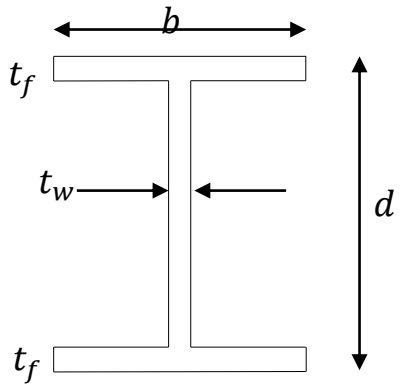

Figure 2.6: I - cross section showing sectional dimensions

The St. Venant torsional constant, J is given as:

$$J = \frac{1}{3}\left(2bt_f^3 + d't_w^3\right) \quad \text{(Galambos 1968)} \qquad 2.2$$

The warping torsional constant is given as:

$$I_\omega = \frac{1}{24}\left(d'^2 b^3 t_f\right) \quad \text{(Galambos 1968, Picard and Beaulieu 1991)} \qquad 2.3$$

Where:

$$d' = d - t_f \qquad 2.4$$

2.6.2 Channel Sections

Structural Stability Research Council, SSRC (1998) gave the formula for calculating the St. Venant torsional constant for a channel cross section. In a similar way, Galambos (1968) and SSRC (1998) in separate works obtained the formula for calculating the warping torsional constant. Furthermore, Galambos (1968) and Seaburg and Carter (1997) in their separate works obtained the formula for calculating the shear center location from the centroid.

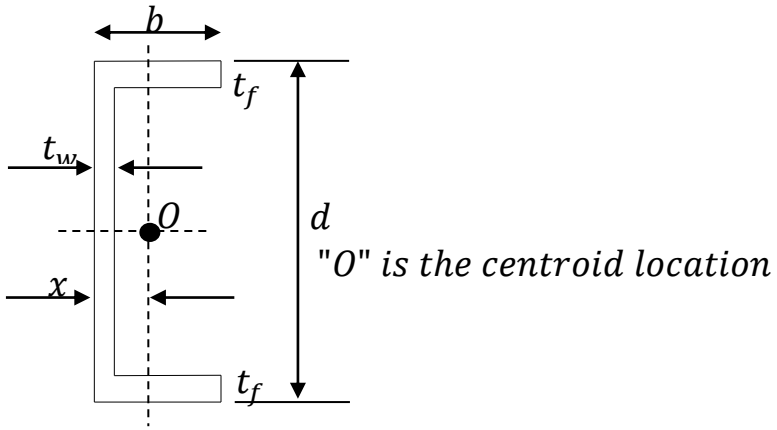

Figure 2.7: Channel cross section showing sectional dimensions

The formula for St. Venant torsional constant is given as:

$$J = \frac{1}{3}\left(2b't_f^3 + d't_w^3\right) \qquad 2.5$$

The warping torsional constant is given as:

$$I_\omega = d'^2 b'^3 t_f \left[\frac{1-3\alpha}{6} + \frac{\alpha^2}{2}\left(1 + \frac{d' t_w}{6 b' t_f}\right)\right] \qquad 2.6$$

The shear constant α, is used for determining the maximum shear stress in the cross section due to an applied shear force. The shear center location from centroid, x_0 is given as:

$$x_0 = x + b'\alpha - \frac{t_w}{2} \qquad 2.7$$

Where:

$$d' = d - t_f \qquad 2.8$$

$$b' = d - \frac{t_w}{2} \qquad 2.9$$

$$\alpha = \frac{1}{2 + \frac{d' t_w}{3 b' t_f}} \qquad 2.10$$

2.6.3 Angle Section

CISC (2002) gave the formula to calculate the St. Venant torsional constant for angle section. Similarly, Bleich (1952) and Picard and Beaulieu (1991) in their separate works determined the formulas for calculating the warping torsional constant.

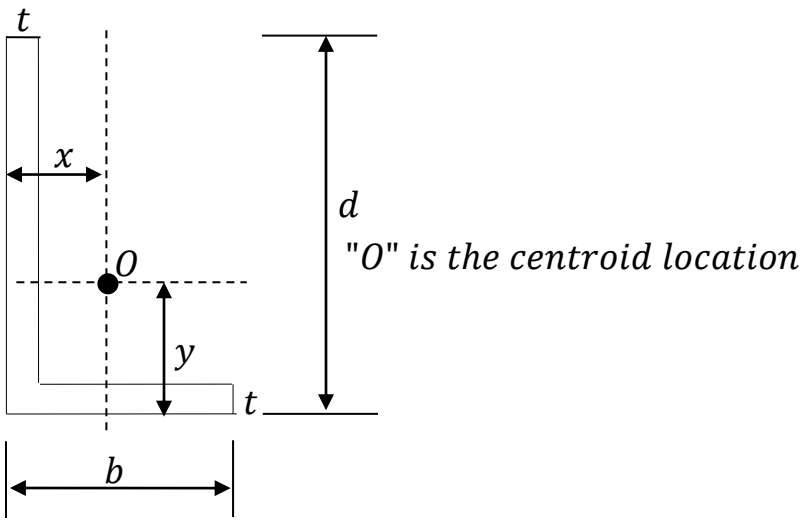

Figure 2.8: Angle cross section showing sectional dimensions

The formula for calculating the St. Venant torsional constant is given as;

$$J = \frac{1}{3}(b' + d')t^3 \qquad 2.11$$

The formula for calculating the warping torsional constant is given as:

$$I_\omega = \frac{t^3}{36}\left(b'^3 + d'^3\right) \qquad 2.12$$

Where:

$$d' = d - \frac{t}{2} \qquad 2.13$$

$$b' = b - \frac{t}{2} \qquad 2.14$$

2.6.4 T-Sections

CISC (2002) gave the formula for calculating the St. Venant torsional constant, J for a T-section. More so, Bleich (1952) and Picard and Beaulieu (1991) in their separate works determined the formula for calculating the warping torsional constant, I_ω.

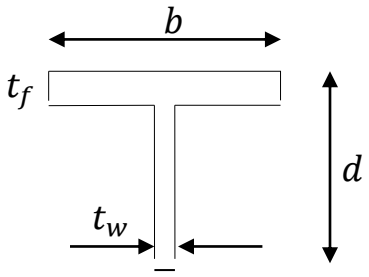

Figure 2.9: T- cross section showing sectional dimensions

The St. Venant torsional constant, J is given as:

$$J = \frac{1}{3}\left(bt_f^3 + d't_w^3\right) \qquad 2.15$$

The warping torsional constant is given as:

$$I_\omega = \frac{b^3 t_f^3}{144} + \frac{d'^3 t_w^3}{36} \qquad 2.16$$

Where:

$$d' = d - \frac{t_f}{2} \qquad 2.17$$

2.7 Methods of Analysis of Thin-Walled Column

Numerous researchers have conducted analyses on thin-walled box columns and related subjects, utilizing various approaches. However, none of them have used the potential energy method based on Rayleigh-Ritz approach to determine the critical buckling load of thin-wall column of open sections. For example, (Nwachukwu, Ezeh, Thomas, Okafor, and Okodugha, 2017) derived the governing equation for the Total Potential Energy Functional (TPEF) for a Doubly Symmetric Single (DSS) cell thin-walled Box Column. (Krolak, Kowal-Michalska, Mania, and Swinlarski, 2009) presented a comprehensive analysis encompassing theory, numerical simulations, and experiments to study the stability and ultimate load of multi-cell thin-walled columns with rectangular and square cross-sections under axial compression. Shanmugam, Richard Liew, and Lee, (1989) proposed a numerical method to investigate the ultimate strength behavior of thin-walled steel box columns subjected to axial loads and biaxial end moments. Ezeh (2010) formulated a theoretical approach based on Vlasov's theory, as modified by Varbanov, to analyze the flexural, torsional-flexural, and torsional-flexural-distortional buckling modes of thin-walled closed columns. Chidolue and Osadebe (2012) also utilized Vlasov's theory to perform torsional-distortional analysis on thin-walled box girder bridges. Chidolue and Aginam (2012) studied the influence of the shape factor on the torsional-flexural-distortional behavior of thin-walled box girder structures, again using Vlasov's theory. Additionally, Ezeh (2009) examined the buckling behavior of axially compressed multi-cell doubly symmetric thin-walled columns, employing Vlasov's theory. The works of Osadebe and Chidolue (2012a), Osadebe and Chidolue (2012b), Osadebe and Ezeh (2009a), and Osadebe and Ezeh (2009b) were also based on Vlasov's method as their analytical framework.

According to Andreassen (2012), there are so many methods recommended for analysis for thin-wall structure. These methods include; (i) finite element method, (ii) finite strip method, (iii) generalized beam theory.

2.7.1 Finite Element Method

This approach presents a way to obtain an approximate solution for a problem that is governed by a set of differential equations. The method involves dividing or discretizing the member into smaller parts, referred to as elements. When dealing with thin-walled members, shell finite elements (SFEM) are typically employed. The displacement field is estimated by combining polynomial shape functions, with each function corresponding to a nodal displacement or rotation. Hughes (2000) gave detailed information concerning this method. It is important to note that this advanced numerical method involves a large number of degrees of freedom.

2.7.2 Finite Strip Method

This approach can be considered as a specialized version of the finite element procedure, and a comparison between the finite element and finite strip methods can be found in Cheung (1976). It is suitable for structures with regular geometric plans and simple loading and boundary conditions. In this method, the member is discretized into strips, which requires the use of simple interpolation polynomials in the transverse direction and continuously differentiable smooth series functions (such as Fourier series) in the longitudinal direction. The strips are rectangular finite elements that span the entire length and involve a smaller number of degrees of freedom compared to equivalent SFEM analyses Cheung and Tham (1998). This simplification offers a powerful advantage over the finite element method.

2.7.3 Generalized Beam Theory

This method possesses a distinctive characteristic whereby the deformed configuration of the member is discretized into various modes of cross-section deformation. These modes can be categorized as global, local (plate), or distortional modes Schardt (1994). Once the modes are determined through cross-section analysis, they are multiplied by an approximate axial amplitude shape function during member analysis, resulting in a conventional axial element interpolation and discretization. The method has been integrated into the freely available software packages GBTUL (Bebiano, Silvestre, and Camotim, 2008) for open cross sections, although it currently lacks the capability to handle closed cross sections. This theory, which is not as widely known as the finite element method and the finite strip method, extends the classical theory by incorporating multiple distortional modes. Consequently, it enables computational analysis of complex distortional problems with fewer degrees of freedom compared to equivalent SFEM analyses. The inclusion of this extension, along with the corresponding longitudinal finite element discretization utilizing an approximated axial amplitude shape function, facilitates faster analysis of intricate dynamic and stability-related issues.

In the field of stability analysis for thin-walled columns of open section, there has been a lack of utilization of the Total potential energy method based on Raleigh-Ritz method. Therefore, it is imperative to advance the current knowledge by developing a specific and unique Total Potential Energy Functional (TPEF) that corresponds to different boundary conditions of singly symmetric section (SSS), doubly symmetric sections (DSS) and generally asymmetric section (ASC) in accordance with the Raleigh-Ritz method. This research relies on the principles of the Raleigh-Ritz energy theory.

2.8 Energy Methods

Energy methods are methods of engineering analysis based on linear elastic behavior and conservation of energy. That is, the work done by external forces equals the energy stored in the structure under load.

Thus, the total potential energy of a system is the summation of the Strain energy of the system and the work done by externally applied forces, Henry (2015).

This is expressed mathematically in Equation (2.18) below:

$$\pi = U + V \tag{2.18}$$

Where U = the average strain energy of the system

V = Work done by externally applied forces

According to Njoku (2018), the use of energy methods become imperative to obtain approximate solutions when it is not possible or very cumbersome to obtain the exact solution of a problem due to the complexity of the problem. The column solution methods based on the energy methods include the Rayleigh, Ritz, and Galarkin-Vlasov (Njoku, 2018).

2.8.1 The Principle of Conservation Of Energy

The fundamental concept of the conservation of energy, as observed and extensively discussed by Reddy (1993) and further elaborated upon by Njoku (2018), emphasizes that within a conservative system wherein no dissipation of energy occurs during the loading process, the amount of work exerted on a body becomes equivalent to the strain energy accumulated by that very body.

2.8.1.1 Strain energy equation of a body

Strain energy is defined as the energy stored in a body due to deformation. The strain energy per unit volume is known as strain energy density and is the area under the stress-strain curve to the point of inelastic deformation. When the applied force is released, the whole system returns to its original shape. It is usually denoted by U.

The strain energy formula is given as (Ibearugbulem, Ezeh, Ettu, 2014),

$$U = F\delta / 2 \quad (2.19)$$

Where,

δ = compression,

F = force applied.

When stress σ is proportional to strain ϵ, the strain energy formula is given by,

$$U = 1/2V\sigma\,\varepsilon \quad (2.20)$$

Where,

σ = stress

ε = strain

V = volume of body

Regarding Young's modulus E, the strain energy formula is given as,

$$U = \sigma^2 / 2E \times V \quad (2.21)$$

Where,

σ = stress,

E = Young's modulus,

V = volume of body.

2.9 Boundary conditions of a column

There are different types of support conditions that a given column could have. These supports or boundaries are as follows: simply-supported, clamped, and free. Shown below in Figure 2.2. is a representation of the boundary conditions.

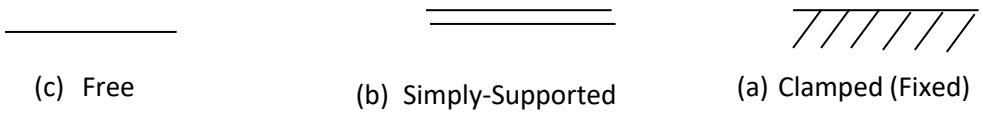

Figure 2.10 Boundary Condition

A column has two ends, and each end could have any of the above listed boundary types. The solution of the column equation requires that the boundary conditions are satisfied.

2.10 Results from Previous Researchers

Past researchers expressed their results in terms of dimensionless parameters. These values for Various researchers are presented for various cases.

2.10.1 Energy formulation for flexural – torsional buckling of thin-walled column with open cross- section

Ike (2018) presented a solution to the problem of flexural – torsional buckling analysis of thin-walled column with open cross-section using energy methods. Thin-walled column with open cross-section of arbitrary slope was considered. The deformation occurring during elastic buckling involves a combination of twisting and bending about two axes of the cross-section. To analyze this phenomenon, the total potential energy functional was formulated by summing the strain energy and the potential energy of the J(z) and v(z), and one rotational displacement, $\theta(z)$.

The values obtained for thin-wall column of different open sections were presented for three cases.

Case 1 Elastic buckling solutions for simply supported thin-walled columns

For thin-walled columns simply supported at the ends z =0 and z = l, the translational displacements in the x and y coordinate directions, and the bending moment about these axes vanish.

The critical buckling load is found as the lowest buckling load and is given as

$$\left(P_{yy_{cr}} - P\right)\left(P_{xx_{cr}} - P\right)\left(P_{\theta_{cr}} - P\right) - \left(P_{yy_{cr}} - P\right)\frac{P^2 x_o^2}{i_o^2} - \left(P_{xx_{cr}} - P\right)\frac{P^2 y_o^2}{i_o^2} = 0 \qquad 2.22$$

where , P is the axial compressive load, $P_{yy_{cr}}$, $P_{xx_{cr}}$ are the critical flexural buckling loads, i_o is the polar radius of gyration of the thin-walled column cross-section with respect to the shear centre. and $P_{\theta_{cr}}$ is the critical torsional buckling load, .

Case 2 Thin-walled column with doubly-symmetric open cross-section

For thin-walled columns with doubly-symmetric open cross-sections, the geometrical centre coincides with the shear centre, and $x_0 = 0$, $y_0 = 0$. The critical buckling equation simplifies to become:

$$\left(P_{yy_{cr}} - P\right)\left(P_{xx_{cr}} - P\right)\left(P_{\theta_{cr}} - P\right) = 0 \qquad 2.23$$

The three roots are the three critical buckling loads, given by:

$$P = P_{xx_{cr}} = \frac{\pi^2 E_{xx}}{i^2} \qquad 2.24$$

Where i is the second moment of inertia, and E is the Young's modulus of the column material

$$P = P_{yy_{cr}} = \frac{\pi^2 E_{yy}}{i^2} \qquad 2.25$$

$$P = P_{\theta_{cr}} = \frac{1}{i_o^2}\left(GI + \frac{\pi^2 E_{ww}}{i^2}\right) \quad 2.27$$

Where G is the shear modulus or modulus of rigidity of the column material, and I is the St Venant torsion constant or the torsional moment of inertia.

The lowest value of P would govern the buckling behavior of the thin-walled column.

Case 3 Thin walled column with singly-symmetric open cross-section

According to Ike (2018), for thin-walled columns with singly-symmetric open crosssections, one of the centroidal coordinates will be zero since the shear centre will lie on one of the axes of the cross-section. When the y axis is the axis of symmetry, the shear centre will lie on the y axis, and $x_0 = 0$, and the buckling equations become:

$$\left(P_{yy_{cr}} - P\right)\left(P_{xx_{cr}} - P\right)\left(P_{\theta_{cr}} - P\right) - \left(P_{xx_{cr}} - P\right)\frac{P^2 y_o^2}{i_o^2} = 0 \quad 2.28$$

This gives:

$$P_{xx_{cr}} - P = 0 \quad 2.29$$

Or

$$P = P_{xx_{cr}} = \frac{\pi^2 E_{xx}}{i^2} \quad 2.30$$

And

$$\left(P_{yy_{cr}} - P\right)\left(P_{\theta_{cr}} - P\right) - \frac{P^2 y_o^2}{i_o^2} = 0 \qquad 2.31$$

Where y_o is the centroidal coordinates of the open cross-section of the thin-walled column

Equation (2.31) is a quadratic equation in P. It has two buckling values corresponding to the two roots (zeros) of the quadratic equation. The equation represents the torsional-flexural buckling equation. When the x axis is the only axis of symmetry, the shear centre will be found on the x axis, $y_0 = 0$, and the characteristic buckling equation becomes:

$$\left(P_{yy_{cr}} - P\right)\left(P_{xx_{cr}} - P\right)\left(P_{\theta_{cr}} - P\right) - \left(P_{yy_{cr}} - P\right)\frac{P^2 x_o^2}{i_o^2} = 0 \qquad 2.32$$

$$\left(P_{yy_{cr}} - P\right)\left\{\left(P_{xx_{cr}} - P\right)\left(P_{\theta_{cr}} - P\right) - \frac{P^2 x_o^2}{i_o^2}\right\} = 0 \qquad 2.33$$

Where x_o is the centroidal coordinates of the open cross-section of the thin-walled column

The buckling equations become:

$$P = P_{yy_{cr}} = \frac{\pi^2 E_{yy}}{i^2} \qquad 2.34$$

$$\left(P_{xx_{cr}} - P\right)\left(P_{\theta_{cr}} - P\right) - \frac{P^2 x_o^2}{i_o^2} = 0 \qquad 2.35$$

The governing torsional-flexural buckling load (P_{FT}) is the smaller root of the torsional-flexural buckling equation, and is obtained as:

$$P_{FT} = \frac{1}{2\alpha}\left\{P_{\theta_{cr}} + P_{xx_{cr}} - \sqrt{\left(P_{\theta_{cr}} - P_{xx_{cr}}\right)^2 - 4\alpha P_{\theta_{cr}} P_{xx_{cr}}}\right\} \qquad 2.36$$

Where,

$$\propto = 1 - \left\{\frac{x_o}{i_o}\right\}^2 \qquad 2.37$$

If the x axis is the only axis of symmetry, and

$$P_{FT} = \frac{1}{2\beta}\left\{P_{\theta_{cr}} + P_{yy_{cr}} - \sqrt{\left(P_{\theta_{cr}} - P_{yy_{cr}}\right)^2 - 4\beta P_{\theta_{cr}} P_{yy_{cr}}}\right\} \qquad 2.38$$

Where,

$$\beta = 1 - \left\{\frac{y_o}{i_o}\right\}^2 \qquad 2.39$$

Table 2.1 Summary Of The Literature Review

Reference	Methodology	Objective
Nwachukwu et al. (2017)*Formulation of the Total Potential Energy Functional for a Thin-Walled Box Column Applicable to Raleigh-Ritz Method*	The study formulated the Total Potential Energy Functional (TPEF), facilitating the application of the Rayleigh-Ritz Method (RRM) using polynomial shape functions.	To develop the TPEF for thin-walled box columns, enabling efficient application of the RRM for stability analysis.
Nwachukwu et al. (2021)*Formulation of the Total Potential Energy Functional Relevant to the Stability Analysis of a Doubly Symmetric Single-Cell Thin-Walled Box Column*	Building on the 2017 study, polynomial shape functions were generated for various boundary conditions. Subsequently, TPEFs were formulated for these conditions in doubly symmetric single-cell box columns.	To establish specific TPEFs for DSS thin-walled box columns, supporting RRM-based stability analysis using polynomial shape functions.
Krolak et al. (2009)*Stability and Load-Carrying Capacity of Multi-Cell Thin-Walled Columns of Rectangular Cross-Sections*	Conducted theoretical, numerical, and experimental investigations on the local and global stability of multi-cell orthotropic and isotropic rectangular columns.	To analyze the stability and ultimate load-carrying capacity of multi-cell thin-walled columns under axial compression.
Ezeh (2010)*Buckling Behavior of Axially Compressed Multi-Cell Doubly Symmetric Thin-Walled Columns Using Vlasov's Theory*	Developed a theoretical approach using Vlasov's theory (as modified by Varbanov) to analyze various buckling modes including flexural, torsional-flexural, and distortional.	To achieve better understanding and distinct separation of distortional buckling modes from other instability behaviors.
Chidolue & Osadebe (2012)*Torsional-Flexural Behavior of Thin-Walled Monosymmetric Box-Girder Structures*	Derived differential equations for torsional-distortional behavior based on Vlasov's theory and applied them to analyze single-cell monosymmetric box-girders.	To formulate and apply governing equations for torsional-distortional behavior in thin-walled monosymmetric box-girders.
Chidolue & Aginam (2012)*Effects of Shape Factor on the Torsional-Flexural-Distortional Behavior of Thin-Walled Box-Girder Structures*	Analyzed the effects of sectorial properties using single and double-cell monosymmetric box girders with equivalent enclosed areas and thicknesses.	To identify and explain distortional stress patterns and deformations resulting from shape factor influences and sectorial area laws.
Ike (2018)*Energy Formulation for Flexural-Torsional Buckling of Thin-Walled Columns with Open Cross-Sections*	Used the energy method to formulate the flexural-torsional buckling problem for columns with open cross-sections. Derived the TPEF and applied Euler-Lagrange equations to minimize it.	To analyze flexural-torsional buckling in thin-walled open-section columns using energy principles and variational methods.

2.11 Research Gap

Upon an extensive review of existing literature focused on the torsional-flexural buckling of thin-wall structures, a critical research gap emerges. Notably, there is a conspicuous absence of studies utilizing the potential energy method based on the Rayleigh-Ritz approach to ascertain the critical buckling load in thin-wall columns of open sections.

The potential energy method, specifically employing the Rayleigh-Ritz approach, stands as a promising avenue that has remained unexplored in the current body of research. This method provides a unique perspective, emphasizing energy considerations in the analysis of structural stability.

Despite the method's potential advantages, including its ability to offer comprehensive insights into the behavior of thin-wall structures under various conditions, none of the reviewed studies incorporated this approach. This absence underscores a significant void in the investigation of critical buckling load determination, particularly in the specific context of thin-wall columns with open sections.

The identification of this research gap serves as the cornerstone for the present study. By introducing the potential energy method within the Rayleigh-Ritz framework to solve the problem of torsional-flexural buckling, this research aims to address the noted deficiency and contribute novel insights to the understanding of critical buckling phenomena in thin-wall structures.

CHAPTER THREE

METHODOLOGY

3.1 Determination of the Total Potential Energy Functional for Thin-Walled Column with Open Cross-Section undergoing Torsional-flexural Buckling

The total potential energy functional ($\prod$) for the thin-walled column with open cross-section under torsional-flexural buckling is the sum of the strain energy functional U and the potential energy due to the external compressive load V

$$\Pi = U - V \qquad 3.1$$

The shear centre of the cross-section is chosen as the origin. The x and y coordinate axes are assumed to be coincident with the principal axes of the open cross-section, and the z coordinate axis is the longitudinal axis of the thin-walled column through the shear centre.

This analysis comprises column buckling under the following cases:

i. Pure flexural buckling

ii. Pure torsional buckling

iii. Flexure - torsional buckling

Consider a column with arbitrary cross section as shown on Figure 3.1.

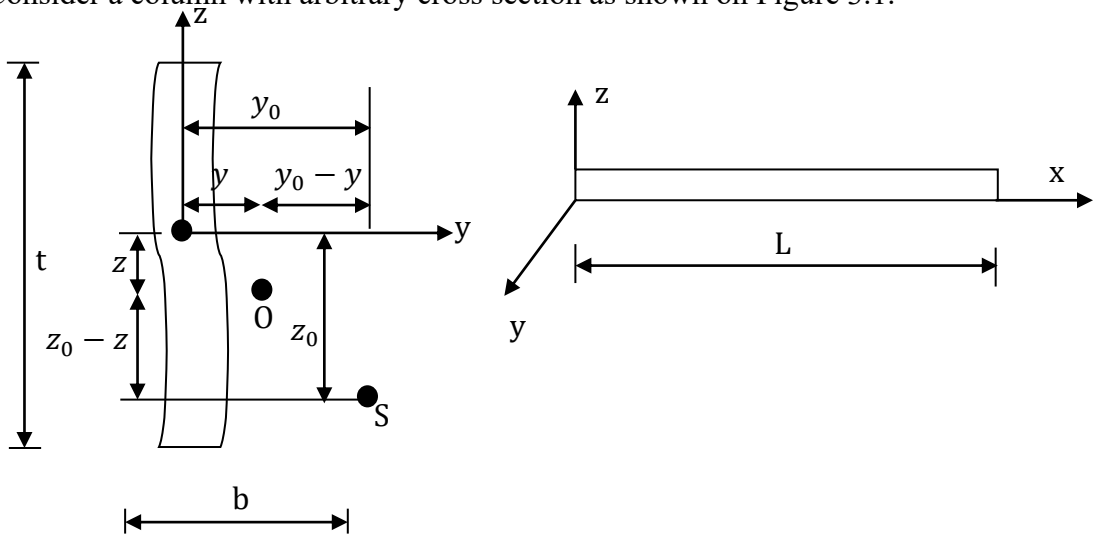

Figure 3.1: Column under axial load

The displacement field include the displacements along x, y and z direction designated as u, v and w. Strain energy and external work for each case shall be treated independently first. The positions of O and S stand for the centroid and shear center respectively.

The displacement of the shear center along y-axis and z- axis are denoted as v and w respectively. On the other hand, the displacement of the centroid along y-axis and z-axisare denoted as v*. w*. The linear space between the shear center and the centroid remains constant after the translational displacement. Thus, the length of OS is the same as

$$w^* = w - (y_0 - y).\emptyset \qquad 3.2$$

$$v^* = v + (z_0 - z).\emptyset \qquad 3.3$$

Where $\emptyset$ is rotation of the cross-section about the shear center O, y_0 and z_0 represent the coordinates of the shear center O

3.1.1 Total Potential Energy Functional for Thin-Walled Column of Open Cross-Sectionin Flexural Buckling

External work in this case is the product of force and the distance travelled by the force. After buckling, the column takes the shape shown on Figure 3.2 below

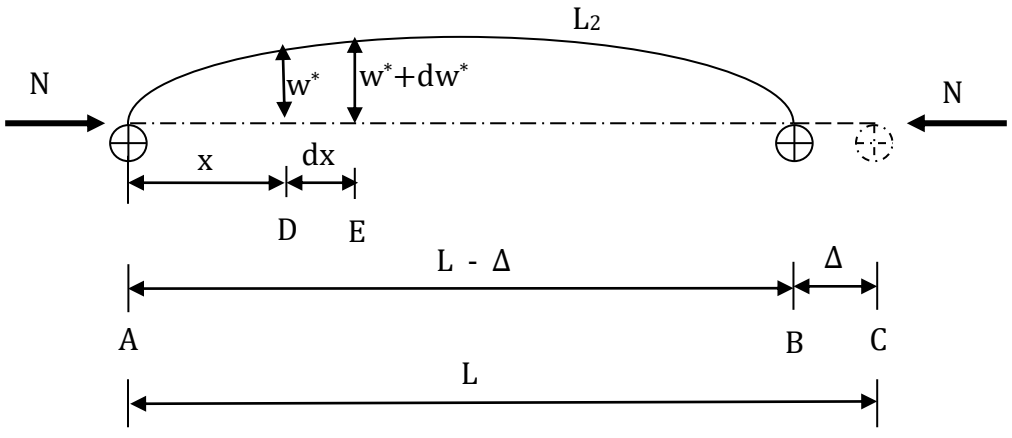

Figure 3.2: A column compressed through Δ and buckled

Due to the axial load, the column buckled and support C moved to a new position, B. The new length of the column is the length of the arc, L_2. The load movement (the distance travelled by the load) is Δ. Let a portion of the column be considered. This portion is defined by points D and E as shown on Figure 3.3. Let this portion be represented on Figure 3.3.

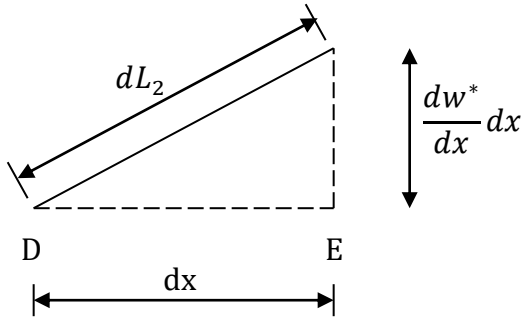

Figure 3.3: Portion of the buckled column between points D and E

From Pythagoras theorem,

$(dL_2)^2 = (dx)^2 + \left(\frac{dw^*}{dx}dx\right)^2$. *That is*:

$(dL_2)^2 = (dx)^2\left[1 + \left(\frac{dw^*}{dx}\right)^2\right]$. *That is*:

$$dL_2 = dx\sqrt{\left[1 + \left(\frac{dw^*}{dx}\right)^2\right]} \qquad 3.4$$

Employing Binomial theorem, Equation 3.4 becomes:

$$dL_2 = dx + \frac{1}{2}\left(\frac{dw^*}{dx}\right)^2 dx \qquad 3.5$$

Let the difference between dL_2 and dx be $d\Delta_z$. That is:

$$d\Delta_z = dL_2 - dx \qquad 3.6$$

Substituting Equation 3.5 into Equation 3.6 gives:

$$d\Delta_z = \frac{1}{2}\left(\frac{dw^*}{dx}\right)^2 dx \qquad 3.7$$

The total change in length of the column after buckling is obtained by integrating Equation 3.7. That is:

$$\Delta_z = \frac{1}{2}\int_0^L \left(\frac{dw^*}{dx}\right)^2 dx \qquad 3.8$$

If the buckling occurred in the y direction, the change in length shall be obtained by modifying Equation 3.8 appropriately as:

$$\Delta_y = \frac{1}{2}\int_0^L \left(\frac{dv^*}{dx}\right)^2 dx \qquad 3.9$$

Total buckling is obtained by adding the buckling in both y and z directions. That is adding Equations 3.8 and 3.9 gives:

$$\Delta = \frac{1}{2}\int_0^L \left[\left(\frac{dv^*}{dx}\right)^2 + \left(\frac{dw^*}{dx}\right)^2\right] dx \qquad 3.10$$

The indefinite summation product of axial stress and buckling caused by it within the domain (cross section area of the column) gives the external work:

$$V = \iint_A \sigma_x \, \Delta \, dA \qquad 3.11$$

From Kirchhoff's assumptions of zero shear strains:

$$\gamma_{xz} = \frac{du_z}{dz} + \frac{dw}{dx} = 0 \qquad 3.12$$

$$\gamma_{xy} = \frac{du_y}{dy} + \frac{dv}{dx} = 0 \qquad 3.13$$

Solving Equations 3.12 and 3.13 gives:

$$u_z = -z\frac{dw}{dx} \qquad 3.14$$

$$u_y = -y\frac{dv}{dx} \qquad 3.15$$

Normal strain in x direction is the first derivative of Equations 3.14 and 3.15 with respect to x:

$$\varepsilon_x.z = -z\frac{d^2w}{dx^2} \qquad 3.16$$

$$\varepsilon_x.z = -y\frac{d^2v}{dx^2} \qquad 3.17$$

Adding Equations 3.16 and 3.17 gives the normal strain along x-axis as:

$$\varepsilon_x = -\left(z\frac{d^2w}{dx^2} + y\frac{d^2v}{dx^2}\right) \qquad 3.18$$

From Hooke's law, stress is mathematically defined as:

$$\sigma_x = E\varepsilon_x = -E\left(z\frac{d^2w}{dx^2} + y\frac{d^2v}{dx^2}\right) \qquad 3.19$$

Strain energy is defined as the product of stress, strain and volume of matter. Thus, average strain energy is:

$$U = \frac{1}{2}\int\int_{b_1}^{b_2}\int_{t_1}^{t_2}\sigma_x\,\varepsilon_x\,dx\,dy\,dz \qquad 3.20$$

Substituting Equations 3.18 and 3.19 into Equation 3.20 gives:

$$U = \frac{E}{2}\int\int_{b_1}^{b_2}\int_{t_1}^{t_2}\left(z\frac{d^2w}{dx^2} + y\frac{d^2v}{dx^2}\right)^2 dx\,dy\,dz$$

That is:

$$U = \frac{E}{2}\int\int_{b_1}^{b_2}\int_{t_1}^{t_2}\left[z^2\left(\frac{d^2w}{dx^2}\right)^2 + 2zy\frac{d^2w}{dx^2} * \frac{d^2v}{dx^2} + y^2\left(\frac{d^2v}{dx^2}\right)^2\right]dx\,dy\,dz$$

That is:

$$U = \frac{E}{2}\int\left[I_z\left(\frac{d^2w}{dx^2}\right)^2 + 2I_{yz}\frac{d^2w}{dx^2} * \frac{d^2v}{dx^2} + I_y\left(\frac{d^2v}{dx^2}\right)^2\right]dx \qquad 3.21$$

Where:

$$I_z = \int_{b_1}^{b_2}\int_{t_1}^{t_2} z^2\,dy\,dz \qquad 3.22$$

$$I_y = \int_{b_1}^{b_2}\int_{t_1}^{t_2} y^2\,dy\,dz \qquad 3.23$$

$$I_{yz} = \int_{b_1}^{b_2} \int_{t_1}^{t_2} yz\, dy\, dz = 0 \qquad 3.24$$

Substituting Equation 3.24 into Equation 3.21 gives:

$$U = \frac{E}{2} \int \left[I_z \left(\frac{d^2 w}{dx^2} \right)^2 + I_y \left(\frac{d^2 v}{dx^2} \right)^2 \right] dx \qquad 3.25a$$

Substituting Equation 3.1 into Equation 3.11 gives:

$$V = \iint_A \sigma_x \frac{1}{2} \int_0^L \left[\left(\frac{dv^*}{dx} \right)^2 + \left(\frac{dw^*}{dx} \right)^2 \right] dx\ dA \qquad 3.25b$$

Where A is cross sectional area

That is:

$$V = \frac{\sigma_x}{2} \iint_A \int_0^L \left[\left(\frac{dv^*}{dx} \right)^2 + \left(\frac{dw^*}{dx} \right)^2 \right] dx\ dA \qquad 3.26$$

Substituting Equations 3.2 and 3.3 into Equation 3.26 gives:

$$V = \frac{\sigma_x}{2} \iint_A \int_0^L \left[\left(\frac{d[v + (z_0 - z).\emptyset]}{dx} \right)^2 + \left(\frac{d[w - (y_0 - y).\emptyset]}{dx} \right)^2 \right] dx\ dA$$

That is:

$$V = \frac{\sigma_x}{2} \iint_A \int_0^L \left[\left(\frac{dv}{dx} + z_0 . \frac{d\emptyset}{dx} - z . \frac{d\emptyset}{dx} \right)^2 + \left(\frac{dw}{dx} - y_0 . \frac{d\emptyset}{dx} + y . \frac{d\emptyset}{dx} \right)^2 \right] dx\ dA$$

That is:

$$V = \frac{\sigma_x}{2} \iint_A \int_0^L \left(\left[\frac{dv}{dx} \right]^2 + 2z_0 . \frac{dv}{dx} \frac{d\emptyset}{dx} - 2z . \frac{dv}{dx} \frac{d\emptyset}{dx} + {z_0}^2 . \left[\frac{d\emptyset}{dx} \right]^2 - 2z_0 z . \left[\frac{d\emptyset}{dx} \right]^2 + z^2 . \left[\frac{d\emptyset}{dx} \right]^2 + \left[\frac{dw}{dx} \right]^2 \right.$$
$$\left. - 2y_0 . \frac{dw}{dx} \frac{d\emptyset}{dx} + 2y . \frac{dw}{dx} \frac{d\emptyset}{dx} + {y_0}^2 . \left[\frac{d\emptyset}{dx} \right]^2 - 2y_0 y . \left[\frac{d\emptyset}{dx} \right]^2 + y^2 . \left[\frac{d\emptyset}{dx} \right]^2 \right) dx\ dA$$

That is:

$$V = \frac{\sigma_x}{2}\iint_A \int_0^L \left(\left[\frac{dv}{dx}\right]^2 + \left[\frac{dw}{dx}\right]^2 + 2[z_0 - z].\frac{dv}{dx}\frac{d\emptyset}{dx} + [{z_0}^2 - 2z_0 z + z^2].\left[\frac{d\emptyset}{dx}\right]^2 + 2[-y_0 + y].\frac{dw}{dx}\frac{d\emptyset}{dx} \right.$$

$$\left. + [{y_0}^2 - 2y_0 y + y^2].\left[\frac{d\emptyset}{dx}\right]^2 \right) dx \; dA$$

That is:

$$V = \frac{\sigma_x}{2}\iint_A \int_0^L \left(\left[\frac{dv}{dx}\right]^2 + \left[\frac{dw}{dx}\right]^2 + 2[z_0 - z].\frac{dv}{dx}\frac{d\emptyset}{dx} - 2[y_0 - y].\frac{dw}{dx}\frac{d\emptyset}{dx} \right.$$

$$\left. + [{y_0}^2 - 2y_0 y + y^2 + {z_0}^2 - 2z_0 z + z^2].\left[\frac{d\emptyset}{dx}\right]^2 \right) dx \; dA$$

If a column section is symmetrical about two axes, the shear center coincides with the centroid, and we have $y_0 = z_0 = 0$.

That is:

$$V = \frac{\sigma_x}{2}\int_0^L \left(A\left[\frac{dv}{dx}\right]^2 + A\left[\frac{dw}{dx}\right]^2 + 2A[z_0 - 0].\frac{dv}{dx}\frac{d\emptyset}{dx} - 2A[y_0 - 0].\frac{dw}{dx}\frac{d\emptyset}{dx} \right.$$

$$\left. + \left[I_y - 2y_0 \times 0 + y^2 + I_z - 2z_0 \times 0 + z^2\right].\left[\frac{d\emptyset}{dx}\right]^2 \right) dx$$

That is:

$$V = \frac{\sigma_x A}{2}\int_0^L \left(\left[\frac{dv}{dx}\right]^2 + \left[\frac{dw}{dx}\right]^2 + \left[{y_0}^2 + {z_0}^2 + \frac{I_y + I_z}{A}\right].\left[\frac{d\emptyset}{dx}\right]^2 - 2y_0.\frac{dw}{dx}\frac{d\emptyset}{dx} \right.$$

$$\left. + 2z_0.\frac{dv}{dx}\frac{d\emptyset}{dx} \right) dx \qquad 3.27$$

Where:

$$I_y = \int_A y^2 \, dA \qquad 3.28$$

$$I_z = \int_A z^2 \, dA \tag{3.29}$$

$$0 = \iint_A y \, dA = \iint_A z \, dA \tag{3.30}$$

Since the case of pure flexural buckling is considered, the torsional work is ignored. Thus, Equation 3.27 becomes:

$$V = \frac{\sigma_x A}{2} \int_0^L \left[\left[\frac{dv}{dx}\right]^2 + \left[\frac{dw}{dx}\right]^2 \right] dx \tag{3.31}$$

Modifying Equation 3.27 gives:

$$V = \frac{\sigma_x A}{2} \int_0^L \left(\left[\frac{dv}{dx}\right]^2 + \left[\frac{dw}{dx}\right]^2 + \frac{1}{A}\left[A{y_0}^2 + A{z_0}^2 + I_y + I_z\right].\left[\frac{d\emptyset}{dx}\right]^2 - 2y_0.\frac{dw}{dx}\frac{d\emptyset}{dx} + 2z_0.\frac{dv}{dx}\frac{d\emptyset}{dx} \right) dx \tag{3.32}$$

$$V = \frac{N_x}{2} \int_0^L \left(\left[\frac{dv}{dx}\right]^2 + \left[\frac{dw}{dx}\right]^2 + \frac{I_0}{A}.\left[\frac{d\emptyset}{dx}\right]^2 - 2y_0.\frac{dw}{dx}\frac{d\emptyset}{dx} + 2z_0.\frac{dv}{dx}\frac{d\emptyset}{dx} \right) dx \tag{3.33}$$

N_x is the external force in x direction.

Ignoring the torsional work in Equation 3.33 since pure flexural buckling is considered gives:

$$V = \frac{N_x}{2} \int_0^L \left[\left[\frac{dv}{dx}\right]^2 + \left[\frac{dw}{dx}\right]^2 \right] dx \tag{3.34}$$

Where:

$$I_0 = A{y_0}^2 + A{z_0}^2 + I_y + I_z \tag{3.35}$$

$$N_x = \sigma_x A \tag{3.36}$$

Total potential energy is the algebraic summation of strain energy and external work:

$$\Pi = U - V \tag{3.37}$$

Substituting Equation 3.25 and 3.34 into Equation 3.37 gives:

$$\Pi = \frac{EI_z}{2}\int\left(\frac{d^2w}{dx^2}\right)^2 dx + \frac{EI_y}{2}\int\left(\frac{d^2v}{dx^2}\right)^2 dx - \frac{N_x}{2}\int_0^L\left(\frac{dw}{dx}\right)^2 dx - \frac{N_x}{2}\int_0^L\left(\frac{dv}{dx}\right)^2 dx \quad 3.38$$

3.1.2 Total Potential Energy Functional for Thin-Walled Column of Open Cross-Section In Torsional Buckling

This case has two sub cases. Case A is a case where ends are allowed to warp, and sub case B, where ends are prevented from warping.

3.1.2.1 Case A: End Free to Warp

Assume the ends of the column in Figure 3.1 are allowed to warp. In this case, one end is restrained from warping while the other is allowed to warp.

This is illustrated on Figure 3.4:

After warping, the flanges normal to the z-axis of the column experienced displacements v_1 and v_2, as shown in Figure 3.4. Similarly, the flanges normal to the y-axis underwent displacements w_1 and w_2, also illustrated in Figure 3.4. These movements sustained angle ∅ at the center of the cross section. From similar triangles:

$$\frac{v_1}{(t_1)} = \frac{v_2}{(t_2)} = \tan\phi \quad 3.39$$

$$\frac{w_1}{(b_1)} = \frac{w_2}{(b_2)} = tan\,\phi \quad 3.40$$

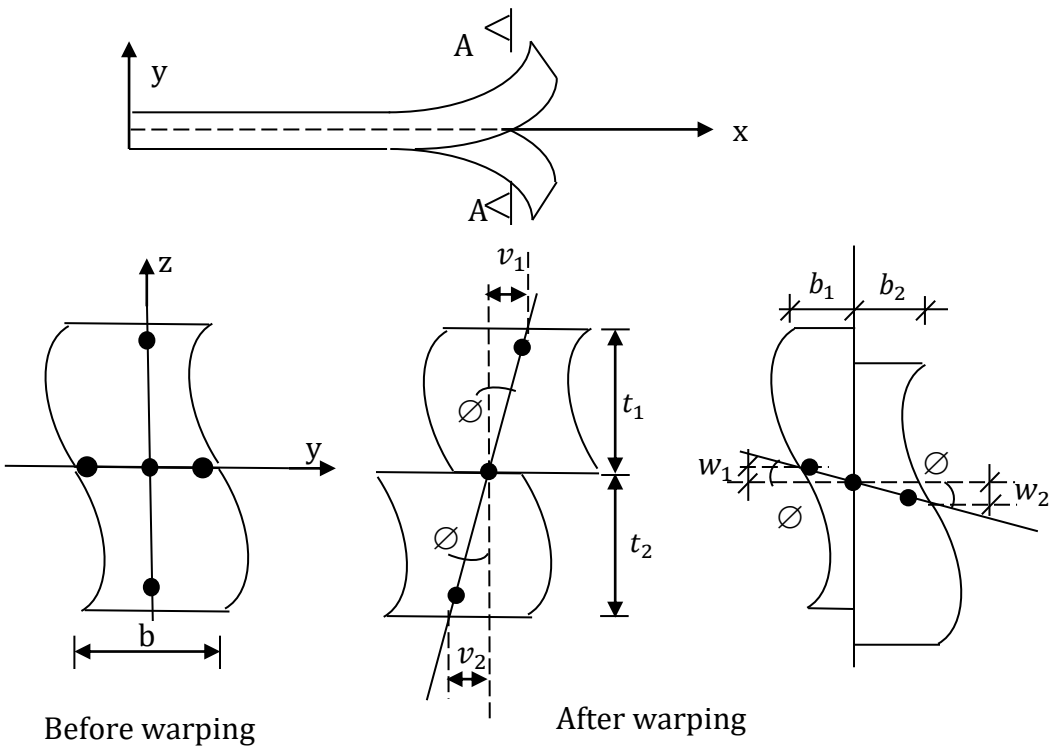

Figure 3.4: One end of column warped

For small deformations,

$$\phi = \tan\phi \qquad 3.41$$

Substituting Equation 3.41 into Equations 3.39 and 3.40 gives:

$$v_i = \mathrm{t}_i\,\phi \qquad 3.42$$

$$w_i = \mathrm{b}_i\,\phi \qquad 3.43$$

Equations 3.42 and 3.43 are rewritten as:

$$v = z\,\phi \qquad 3.44$$

$$w = y\,\phi \qquad 3.45$$

From Kirchhoff's assumptions of zero shear strains:

$$\gamma_{xy} = \frac{du_y}{dy} + \frac{dv}{dx} = 0 \qquad 3.46$$

Solving Equation 3.46 gives:

$$u_y = -y\frac{dv}{dx} \qquad 3.47$$

Substituting Equation 3.42 into Equation 3.47 gives:

$$u_y = -y\,\mathrm{t}_i\frac{d\phi}{dx} \qquad 3.48$$

Similarly if the warping of the flanges moves in z direction,

$$u_z = -z\mathrm{b}_i\frac{d\phi}{dx} \qquad 3.49$$

Axial displacement is the summation of Equations 3.48 and 3.49. That is:

$$u = u_y + u_z = -y\,\mathrm{t}_i\frac{d\phi}{dx} - z\mathrm{b}_i\frac{d\phi}{dx} = -(y\,\mathrm{t}_i + z\mathrm{b}_i)\frac{d\phi}{dx} \qquad 3.50$$

Normal strain in x direction is the first derivative of Equations 3.50 with respect to x:

$$\varepsilon_x = -(y\,\mathrm{t}_i + z\mathrm{b}_i)\frac{d^2\phi}{dx^2} \qquad 3.51$$

The twist (shear strain around x-axis) is obtained by adding the first derivatives of w and v with respect to x. That is the summation of the first derivatives of Equations 3.44 and 3.45 with respect to x. That is:

$$\gamma_s = \varepsilon_{zx} + \varepsilon_{yx} \qquad 3.52$$

Where γ_s is shear strain around x-axis

The first derivatives of Equation 3.44 and 3.45 with respect to x are:

$$\varepsilon_{yx} = \frac{dv}{dx} = z\frac{d\phi}{dx} \qquad 3.53$$

$$\varepsilon_{zx} = \frac{dw}{dx} = y\frac{d\phi}{dx} \qquad 3.54$$

Substituting Equations 3.53 and 3.54 into Equation 3.52 gives:

$$\gamma_s = (y+z)\frac{d\phi}{dx} \qquad 3.55$$

From Hooke's law, normal and shear stresses are mathematically defined as:

$$\sigma_x = E\varepsilon_x = -E(y\,\mathrm{t}_i + z\mathrm{b}_i)\frac{d^2\phi}{dx^2} \qquad 3.56$$

$$\tau_s = G\gamma_s = G(y+z)\frac{d\phi}{dx} \qquad 3.57$$

Where τ_s is shear stress

Strain energy is defined as the product of stress, strain and volume of matter. Thus, average strain energy is:

$$U_y = \frac{1}{2}\int\int_{b_1}^{b_2}\int_{t_1}^{t_2}(\sigma_x\varepsilon_x + \tau_s\gamma_s)\,dxdydz \qquad 3.58$$

Substituting equations 3.51, 3.52, 3.55 and 3.56 into equation 3.58 gives:

$$U = \frac{1}{2}\int\int_{b_1}^{b_2}\int_{t_1}^{t_2}\left[E(y\,\mathrm{t}_i + z\mathrm{b}_i)^2\left(\frac{d^2\phi}{dx^2}\right)^2 + G(y+z)^2\left(\frac{d\phi}{dx}\right)^2\right]dx\,dydz \qquad 3.59$$

$$U = \frac{E}{2}\int\left(\frac{d^2\phi}{dx^2}\right)^2 dx\int_{b_1}^{b_2}\int_{t_1}^{t_2}(y\,\mathrm{t}_i + z\mathrm{b}_i)^2\;dydz$$

$$+\frac{G}{2}\int\left(\frac{d\phi}{dx}\right)^2 dx\int_{b_1}^{b_2}\int_{t_1}^{t_2}(y+z)^2\;dydz \qquad 3.60$$

$$U = \frac{EI_\omega}{2}\int\left(\frac{d^2\phi}{dx^2}\right)^2 dx + \frac{GJ}{2}\int\left(\frac{d\phi}{dx}\right)^2 dx \qquad 3.61$$

Where: the warping torsional constant I_w and St. Venant torsional constant J are defined as:

$$I_\omega = \int_{b_1}^{b_2}\int_{t_1}^{t_2}(y\,\mathrm{t}_i + z\mathrm{b}_i)^2\,dydz \qquad 3.62$$

$$J = \int_{b_1}^{b_2}\int_{t_1}^{t_2}(y+z)^2\,dydz \qquad 3.63$$

From Equation 3.15:

$\frac{u}{y} = -\frac{dv}{dx}$. $That\ is$:

$$\left(\frac{u}{y}\right)^2 = \left(\frac{dv}{dx}\right)^2 \qquad 3.64$$

Substituting Equation 3.64 into Equation 3.27 gives:

$$V_y = \frac{1}{2}\int_0^L \int_{t_1}^{t_2} N_x \left(\frac{u}{y}\right)^2 dxdz \qquad 3.65$$

Rearranging Equation 3.48 gives:

$$\frac{u}{y} = -\mathrm{t}_i \frac{d\phi}{dx} \qquad 3.66$$

Substituting Equation 3.66 into Equation 3.65 gives:

$$V_y = \frac{N}{2}\int_0^L \int_{t_1}^{t_2} N_x {\mathrm{t}_i}^2 \left(\frac{d\phi}{dx}\right)^2 dxdz = \frac{1}{2}\int_0^L \frac{N\mathrm{I}_0}{\mathrm{A_c}} \left(\frac{d\phi}{dx}\right)^2 dx\ .That\ is:$$

$$V_y = \frac{N}{2}\frac{\mathrm{I}_0}{\mathrm{A_c}}\int_0^L \left(\frac{d\phi}{dx}\right)^2 dx \qquad 3.67$$

Where:

$$\frac{N\mathrm{I}_0}{\mathrm{A_c}} = \int_{t_1}^{t_2} N_x {\mathrm{t}_i}^2\, dz \qquad 3.68$$

Where: A_c is the area of the cross section.

I_o is the polar moment of inertia of the cross-section about the longitudinal axis passing through the shear center O.

Adding equation 3.61 and 3.67 gives the total potential energy:

$$\Pi = \frac{EI_\omega}{2}\int \left(\frac{d^2\phi}{dx^2}\right)^2 dx - \frac{N}{2}\frac{\mathrm{I}_0}{\mathrm{A_c}}\int_0^L \left(\frac{d\phi}{dx}\right)^2 dx \qquad 3.69$$

3.1.2.2 Case B: Ends Prevented from Warp

This is a case where only twisting is applied with ends prevented from warping. Consider, for instance if the column in Figure 3.1 is assumed to be circular bar as shown on Figure 3.5.

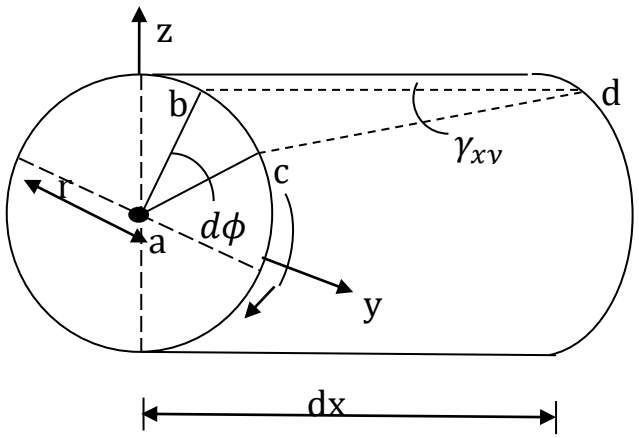

Figure 3.5: Small length of a circular shaft undergoing twisting

After twisting, point b of the shaft moved through an angle ∅ to a new position, c. This caused shearing of the shaft through angle γ as shown on Figure 3.5. Since, the deformation is small, the angles (twist and shear strain) are defined as:

$$d\phi = \sin d\phi = \frac{bc}{ac} = \frac{bc}{r} \qquad 3.70$$

$$\gamma_{xy} = \sin \gamma_{xy} = \frac{bc}{bd} = \frac{bc}{dx} \qquad 3.71$$

From Equations 3.70 and 3.71, it is gathered that:

$$\gamma_{xy} = r\frac{d\phi}{dx} \qquad 3.72$$

Now, consider r to be y. This makes Equation 3.72 to be:

$$\gamma_{xy} = y\frac{d\phi}{dx} \qquad 3.73$$

On the other hand let r be z. This then makes Equation 3.72 to become:

$$\gamma_{xz} = z\frac{d\phi}{dx} \qquad 3.74$$

From Hooke's law, shear stress is mathematically defined as:

$$\tau_{xy} = G\gamma_{xy} \qquad 3.75$$

Substituting Equation 3.73 into Equation 3.75 gives:

$$\tau_{xy} = G.y\,.\ \frac{d\phi}{dx} \qquad 3.76$$

Where G is shear modulus

Strain energy is defined as the product of stress, strain and volume of matter. Thus, average strain energy is:

$$U_{xy} = \frac{1}{2}\int\int\left[\int \tau_{xy}\,.\gamma_{xy}\,dy\right]dx\,dz \qquad 3.77$$

Substituting Equations 3.73 and 3.76 into Equation 3.77 gives:

$$U_{xy} = \left[\frac{1}{2}\int\int G\left(\frac{d\phi}{dx}\right)^2 dx\,dz\right].\left[\int y^2\,dy\right].\ That\ is:$$

$$U_{xy} = G\left[\frac{1}{2}\int\left(\frac{d\phi}{dx}\right)^2 dx\right]\left[\int dz\right].\left[\int y^2\,dy\right].\quad That\ is:$$

$$U_{xy} = \frac{GJ}{2}\int\left(\frac{d\phi}{dx}\right)^2 dx \qquad 3.78$$

Where J is the St. Venant torsional constant defined as:

$$J = \int\int y^2\,dydz \qquad 3.79$$

The total potential energy of a column subject to torsional buckling is obtained by adding equations 3.69 and 3.78:

$$\Pi = \frac{EI_\omega}{2}\int\left(\frac{d^2\phi}{dx^2}\right)^2 dx - \frac{N_x}{2}\frac{\mathrm{I_0}}{\mathrm{A_c}}\int_0^L\left(\frac{d\phi}{dx}\right)^2 dx + \frac{GJ}{2}\int\left(\frac{d\phi}{dx}\right)^2 dx \qquad 3.80$$

3.1.3 Total Potential Energy Functional for Thin-Walled Column of Open Cross-Section in Torsional-flexural Buckling

The strain energy for this case is obtained by adding Equations 3.25, 3.61 and 3.78:

$$U = \frac{EI_z}{2}\int\left(\frac{d^2w}{dx^2}\right)^2 dx + \frac{EI_y}{2}\int\left(\frac{d^2v}{dx^2}\right)^2 dx + \frac{EI_\omega}{2}\int\left(\frac{d^2\phi}{dx^2}\right)^2 dx + \frac{GJ}{2}\int\left(\frac{d\phi}{dx}\right)^2 dx \qquad 3.81$$

Where:

$$I_z = \iint_A z^2\ dA \qquad 3.82$$

$$I_y = \iint_A y^2\ dA \qquad 3.83$$

$$I_\omega = \iint_A (y\,\mathrm{t}_i + z\mathrm{b}_i)^2\ dA \qquad 3.84$$

$$J = \iint_A (y+z)^2\ dA \qquad 3.85$$

Subtracting Equation 3.33 from Equation 3.81 gives the total potential energy functional:

$$\Pi = \frac{E}{2}\int\left[I_z\left(\frac{d^2w}{dx^2}\right)^2 + I_y\left(\frac{d^2v}{dx^2}\right)^2 + I_\omega\left(\frac{d^2\phi}{dx^2}\right)^2 + \frac{GJ}{E}\left(\frac{d\phi}{dx}\right)^2 - \frac{N_x}{E}\left(\frac{dv}{dx}\right)^2 - \frac{N_x}{E}\left(\frac{dw}{dx}\right)^2 - \frac{N_x I_0}{EA}\cdot\left(\frac{d\emptyset}{dx}\right)^2 + \frac{2y_0N_x}{E}\cdot\frac{dw}{dx}\cdot\frac{d\emptyset}{dx} - \frac{2z_0N_x}{E}\cdot\frac{dv}{dx}\cdot\frac{d\emptyset}{dx}\right] dx \qquad 3.86$$

Where:

$$I_0 = Ay_0{}^2 + Az_0{}^2 + I_y + I_z \qquad 3.87$$

Equation 3.86 can be written in non-dimensional coordinate, R (where: R = x/L) as:

$$\Pi = \frac{E}{2L^3}\int \left[I_z \left(\frac{d^2w}{dR^2}\right)^2 + I_y \left(\frac{d^2v}{dR^2}\right)^2 + I_\omega \left(\frac{d^2\phi}{dR^2}\right)^2 + \frac{GJL^2}{E}\left(\frac{d\phi}{dR}\right)^2 - \frac{N_x L^2}{E}\left(\frac{dv}{dR}\right)^2 - \frac{N_x L^2}{E}\left(\frac{dw}{dR}\right)^2 \right.$$

$$\left. - \frac{N_x I_0 L^2}{EA}.\left(\frac{d\emptyset}{dR}\right)^2 + \frac{2y_0 N_x L^2}{E}.\frac{dw}{dR}.\frac{d\emptyset}{dR} - \frac{2z_0 N_x L^2}{E}.\frac{dv}{dR}.\frac{d\emptyset}{dR}\right] dR \qquad 3.88$$

3.2 Determination of the Differential Equation for the Flexural Torsional Buckling Analysis of Thin-Walled Columns with Open Cross-Sections

The differential equations shall be obtained by minimizing the total potential energy functional with respect to the displacement functions. v, w and ϕ.

Minimizing Equation 3.88 with respect to v gives:

$$\frac{d\Pi}{dv} = 0 = \frac{E}{2L^3}\int_x \left(2I_y \frac{d^4v}{dR^4} + I_z[0]^2 + I_\omega[0]^2 + \frac{L^2}{E}\left[GJ - N_x\frac{I_0}{A}\right](0)^2 - \frac{N_x L^2}{E}[0]^2 - 2\frac{N_x L^2}{E}\frac{d^2v}{dR^2}\right.$$

$$\left. + 2y_0 .\frac{N_x L^2}{E}.0 - 2z_0 .\frac{N_x L^2}{E}.\frac{d^2\emptyset}{dR^2}\right) dR$$

That is:

$$\frac{E}{2L^3}\int_x \left(2I_y \frac{d^4v}{dR^4} - 2\frac{N_x L^2}{E}\frac{d^2v}{dR^2} - 2z_0 .\frac{N_x L^2}{E}.\frac{d^2\emptyset}{dR^2}\right) dR = 0$$

That is:

$$\frac{I_y E}{N_x L^2}\left(\frac{d^4v}{dR^4}\right) - \frac{d^2v}{dR^2} - z_0 .\frac{d^2\emptyset}{dR^2} = 0 \qquad 3.89$$

Minimizing Equation 3.88 with respect to w gives:

$$\frac{d\Pi}{dw} = 0 = \frac{E}{2L^3}\int_x \left(I_y[0]^2 + 2I_z \frac{d^4w}{dR^4} + I_\omega[0]^2 + \frac{L^2}{E}\left[GJ - N_x\frac{I_0}{A}\right](0)^2 - 2\frac{N_x L^2}{E}\frac{d^2w}{dR^2} - \frac{N_x L^2}{E}[0]^2\right.$$

$$\left. + 2y_0 .\frac{N_x L^2}{E}.\frac{d^2\emptyset}{dR^2} - 2z_0 .\frac{N_x L^2}{E}.0\right) dR$$

That is:

$$\frac{E}{2L^3}\int_x \left(0 + 2I_z\frac{d^4w}{dR^4} + 0 + 0 + 2\frac{N_xL^2}{E}\frac{d^2w}{dR^2} - 0 + 2y_0\,.\frac{N_xL^2}{E}.\frac{d^2\emptyset}{dR^2} - \ 0\right)dR = 0$$

That is:

$$0 + 2I_z\frac{d^4w}{dR^4} + 0 + 0 + 2\frac{N_xL^2}{E}\frac{d^2w}{dR^2} - 0 + 2y_0\,.\frac{N_xL^2}{E}.\frac{d^2\emptyset}{dR^2} - \ 0 = 0$$

That is:

$$2I_z\frac{d^4w}{dR^4} + 2\frac{N_xL^2}{E}\frac{d^2w}{dR^2} + 2y_0\,.\frac{N_xL^2}{E}.\frac{d^2\emptyset}{dR^2} = 0$$

That is:

$$\frac{I_zE}{N_xL^2}\frac{d^4w}{dR^4} + \frac{d^2w}{dR^2} + y_0.\frac{d^2\emptyset}{dR^2} = 0 \qquad 3.90$$

Minimizing Equation 3.88 with respect to ϕ gives:

$$\frac{d\Pi}{d\emptyset} = 0 = \frac{E}{2L^3}\int_x \left(I_y[0]^2 + I_z[0]^2 + 2I_\omega\frac{d^4\emptyset}{dR^4} + 2\frac{L^2}{E}\left[GJ - N_x\frac{I_0}{A}\right]\frac{d^2\emptyset}{dR^2} - \frac{N_xL^2}{E}[0]^2 - \frac{N_xL^2}{E}[0]^2 + 2y_0\,.\frac{N_xL^2}{E}.\frac{d^2w}{dR^2} - 2z_0\,.\frac{N_xL^2}{E}.\frac{d^2v}{dR^2}\right)dR$$

That is:

$$\frac{E}{2L^3}\int_x \left(0 + 0 + 2I_\omega\frac{d^4\emptyset}{dR^4} + 2\frac{L^2}{E}\left[GJ - N_x\frac{I_0}{A}\right]\frac{d^2\emptyset}{dR^2} - 0 - 0 + 2y_0\,.\frac{N_xL^2}{E}.\frac{d^2w}{dR^2} - 2z_0\,.\frac{N_xL^2}{E}.\frac{d^2v}{dR^2}\right)dR = 0$$

That is:

$$2I_\omega\frac{d^4\emptyset}{dR^4} + 2\frac{L^2}{E}\left[GJ - N_x\frac{I_0}{A}\right]\frac{d^2\emptyset}{dR^2} + 2y_0\,.\frac{N_xL^2}{E}.\frac{d^2w}{dR^2} - 2z_0\,.\frac{N_xL^2}{E}.\frac{d^2v}{dR^2} = 0$$

That is:

$$\frac{I_\omega E}{N_x L^2}\frac{d^4\emptyset}{dR^4}+\left[\frac{GJ}{N_x}-\frac{I_0}{A}\right]\frac{d^2\emptyset}{dR^2}+y_0\cdot\frac{d^2w}{dR^2}-z_0\cdot\frac{d^2v}{dR^2}=0 \qquad 3.91$$

Solving Equations 3.89. 3.90 and 3.91 simultaneously gave the following relations:

$$\emptyset = g_1.v \qquad 3.92$$

$$\emptyset = g_2.w \qquad 3.93$$

$$v = g_3.w \qquad 3.94$$

Where: $g_1, g_2$and g_3 are constants that will be determined later.

Substituting Equations 3.93 and 3.94 into Equation 3.88 gives:

$$\Pi=\frac{E}{2L^3}\int\left[I_z\left(\frac{d^2w}{dR^2}\right)^2+I_y.{g_3}^2\left(\frac{d^2w}{dR^2}\right)^2+I_\omega.{g_2}^2\left(\frac{d^2w}{dR^2}\right)^2+\frac{GJL^2}{E}.{g_2}^2\left(\frac{dw}{dR}\right)^2-\frac{N_xL^2}{E}.{g_3}^2\left(\frac{dw}{dR}\right)^2\right.$$
$$-\frac{N_xL^2}{E}\left(\frac{dw}{dR}\right)^2-\frac{N_xL^2I_0}{EA}.{g_2}^2\left(\frac{dw}{dR}\right)^2+\frac{2.g_2y_0N_xL^2}{E}.\left(\frac{dw}{dR}\right)^2$$
$$\left.-\frac{2.g_2g_3z_0N_xL^2}{E}.\left(\frac{dw}{dR}\right)^2\right]dR$$

That is:

$$\Pi=\frac{E}{2L^3}\int\left[\left(\frac{d^2w}{dR^2}\right)^2\left(I_z+I_y.{g_3}^2+I_\omega.{g_2}^2\right)\right.$$
$$+\left(\frac{dw}{dR}\right)^2\left(\frac{GJL^2}{E}.{g_2}^2-\frac{N_xL^2}{E}.{g_3}^2-\frac{N_xL^2}{E}-\frac{N_xL^2I_0}{EA}.{g_2}^2+\frac{2.g_2y_0N_xL^2}{E}\right.$$
$$\left.\left.-\frac{2.g_2g_3z_0N_xL^2}{E}\right)\right]dR$$

That is:

$$\Pi = \frac{E}{2L^3}\int \left[\left(\frac{d^2w}{dR^2}\right)^2 \left(I_z + I_y.{g_3}^2 + I_\omega.{g_2}^2\right)\right.$$

$$+ \left(\frac{dw}{dR}\right)^2 \left(\frac{GJ}{N_x}.{g_2}^2 - {g_3}^2 - 1 - \frac{I_0}{A}.{g_2}^2 + 2.g_2 y_0\right.$$

$$\left.\left. - 2.g_2 g_3 z_0\right).\frac{N_x L^2}{E}\right] dR \qquad 3.95$$

Equation 3.95 can be written as:

$$\Pi = \frac{E}{2L^3}\int \left[\left(\frac{d^2w}{dR^2}\right)^2 I_T + \left(\frac{dw}{dR}\right)^2.\frac{N_T L^2}{E}\right] dR \qquad 3.96$$

Where:

$$I_T = I_z + I_y.{g_3}^2 + I_\omega.{g_2}^2 \qquad 3.97$$

$$N_T = N_x\left(\frac{GJ}{N_x}.{g_2}^2 - {g_3}^2 - 1 - \frac{I_0}{A}.{g_2}^2 + 2.g_2 y_0 - 2.g_2 g_3 z_0\right) \qquad 3.98$$

Equation 3.96 can be written as:

$$\Pi = \frac{EI_T}{2L^3}\int \left[\left(\frac{d^2w}{dR^2}\right)^2 + \left(\frac{dw}{dR}\right)^2.\frac{N_T L^2}{EI_T}\right] dR \qquad 3.99$$

Minimizing Equation 3.99 with respect to w gives the governing Equation of the thin-walled open cross section column undergoing torsional-flexural buckling as:

$$\frac{d\Pi}{dw} = \frac{EI_T}{L^3}\int \left[\frac{d^4w}{dR^4} + \frac{d^2w}{dR^2}.\frac{N_T L^2}{EI_T}\right] dR = 0 \qquad 3.100$$

For Equation 3.100 to be true, its integrand must be zero. That is:

$$\frac{d^4w}{dR^4} + \frac{d^2w}{dR^2}.\frac{N_T L^2}{EI_T} = 0 \qquad 3.101$$

3.3 Determination of Buckling Load Formulas

The ready solution for Equation 3.101 is given by (Timoshenko & Gere, 1961) as:

$$w = a_1 + a_2R + a_3\,cos\,BR + a_4\,sin\,BR \qquad 3.102$$

Equation 3.102 can be written in short form as:

$$w = hB_2 \qquad 3.103$$

Where:

$$B_2 = [a_1 a_2 a_3 a_4]^T \qquad 3.104$$

$$h = [1 \;\; R \;\; cos\,BR \; sin\,BR] \qquad 3.105$$

Substituting Equation 3.103 into Equations 3.93 and 3.94 respectively gave:

$$\emptyset = g_2.hB_2 = hB_3 \qquad 3.106$$

$$v = g_3.hB_2 = hB_1 \qquad 3.107$$

Rearranging Equations 3106 and 3.107 gives:

$$B_3 = g_2.B_2 \qquad 3.108$$

$$B_1 = g_3.B_2 \qquad 3.109$$

Substituting Equation 3.103 into Equation 3.95 gives:

$$\Pi = \frac{E}{2L^3}\int \left[\left(\frac{d^2h}{dR^2}\right)^2 {B_2}^2.\left(I_z + I_y.{g_3}^2 + I_\omega.{g_2}^2\right)\right.$$

$$\left. + \left(\frac{dh}{dR}\right)^2 {B_2}^2.\left(\frac{GJ}{N_x}.{g_2}^2 - {g_3}^2 - 1 - \frac{I_0}{A}.{g_2}^2 + 2.g_2y_0 - 2.g_2g_3z_0\right).\frac{N_xL^2}{E}\right] dR$$

That is:

$$\Pi = \frac{E}{2L^3}\int \left[\left(\frac{d^2h}{dR^2}\right)^2 \left(I_z.{B_2}^2 + I_y.{g_3}^2{B_2}^2 + I_\omega.{g_2}^2{B_2}^2\right)\right.$$

$$+ \left(\frac{dh}{dR}\right)^2 \left(\frac{GJ}{N_x}.{g_2}^2{B_2}^2 - {g_3}^2{B_2}^2 - {B_2}^2 - \frac{I_0}{A}.{g_2}^2{B_2}^2 + 2.g_2{B_2}^2 y_0\right.$$

$$\left.\left. - 2.g_2 g_3 {B_2}^2 z_0\right).\frac{N_x L^2}{E}\right] dR \qquad 3.110$$

Substituting Equations 3.108 and 3.109 into Equation 3.10 gives:

$$\Pi = \frac{E}{2L^3}\int \left[\left(\frac{d^2h}{dR^2}\right)^2 \left(I_z.{B_2}^2 + I_y.{B_1}^2 + I_\omega.{B_3}^2\right)\right.$$

$$\left. + \left(\frac{dh}{dR}\right)^2 \left(\frac{GJ}{N_x}.{B_3}^2 - {B_1}^2 - {B_2}^2 - \frac{I_0}{A}.{B_3}^2 + 2.B_2B_3y_0 - 2.B_1B_3z_0\right).\frac{N_xL^2}{E}\right] dR$$

That is:

$$\Pi = \frac{E}{2L^3}\int \left[\left(\frac{d^2h}{dR^2}\right)^2 \left(I_y.{B_1}^2 + I_z.{B_2}^2 + I_\omega.{B_3}^2\right)\right.$$

$$\left. + \left(\frac{dh}{dR}\right)^2 \left(-{B_1}^2 - {B_2}^2 + \left[\frac{GJ}{N_x}.-\frac{I_0}{A}\right].{B_3}^2 - 2.B_1B_3z_0 + 2.B_2B_3y_0\right).\frac{N_xL^2}{E}\right] dR$$

That is:

$$\Pi = \frac{E}{2L^3}\int_0^1 \left[\left(\frac{d^2h}{dR^2}\right)^2 \left(I_y.{B_1}^2 + I_z.{B_2}^2 + I_\omega.{B_3}^2\right)\right.$$

$$- \left(\frac{dh}{dR}\right)^2 \left({B_1}^2 + {B_2}^2 + \left[\frac{I_0}{A} - \frac{GJ}{N_x}\right].{B_3}^2 + 2.B_1B_3z_0\right.$$

$$\left.\left. - 2.B_2B_3y_0\right).\frac{N_xL^2}{E}\right] dR \qquad 3.111$$

In a symbolized form, Equation 3.111 is written as:

$$\Pi = \frac{E}{2L^3}\Big[k_{RR}.\left(I_y.{B_1}^2 + I_z.{B_2}^2 + I_\omega.{B_3}^2\right)$$

$$- k_R\left({B_1}^2 + {B_2}^2 + \left[\frac{I_0}{A} - \frac{GJ}{N_x}\right].{B_3}^2 + 2.B_1B_3z_0 - 2.B_2B_3y_0\right).\frac{N_xL^2}{E}\Big] \qquad 3.112$$

Rewriting Equation 3.112 gives:

$$\Pi = \frac{E}{2L^3}\Bigg({B_1}^2 I_y k_{RR} + {B_2}^2 I_z k_{RR} + {B_3}^2 I_\omega k_{RR} + {B_3}^2 \frac{L^2}{E} GJ k_R - {B_3}^2 \frac{N_xL^2}{E}.\frac{I_0}{A}k_R - {B_2}^2 \frac{N_xL^2}{E}k_R$$

$$- {B_1}^2 \frac{N_xL^2}{E}k_R + 2B_2B_3y_0\,.\frac{N_xL^2}{E}k_R - 2B_1B_3z_0\,.\frac{N_xL^2}{E}k_R\Bigg) \qquad 3.113$$

Rewriting Equation 3.113 by collecting like terms (B_1 together, B_2 together and B_3 together) gives:

$$\Pi = \frac{E}{2L^3}\Bigg({B_1}^2\left[I_y k_{RR} - \frac{N_xL^2}{E}k_R\right] + {B_2}^2\left[I_z k_{RR} - \frac{N_xL^2}{E}k_R\right] + {B_3}^2\left[I_\omega k_{RR} + \frac{L^2}{E}GJk_R - \frac{N_xL^2}{E}.\frac{I_0}{A}k_R\right]$$

$$+ 2B_2B_3y_0\,.\frac{N_xL^2}{E}k_R$$

$$- 2B_1B_3z_0\,.\frac{N_xL^2}{E}k_R\Bigg) \qquad 3.114$$

Where, $k_R = \left(\frac{dh}{dR}\right)^2 dR$

$$k_{RR} = \left(\frac{d^2h}{dR^2}\right)^2 dR$$

3.3.1 Case of General Unsymmetrical Open Section

Minimizing Equation 3.114 with respect to B_1 gives:

$$\frac{d\Pi}{dB_1} = \frac{E}{2L^3}\left(2B_1\left[I_y k_{RR} - \frac{N_xL^2}{E}k_R\right] - 2B_3z_0\,.\frac{N_xL^2}{E}k_R\right) = 0$$

That is:

$$B_1\left[I_y k_{RR} - \frac{N_xL^2}{E}k_R\right] - B_3z_0\,.\frac{N_xL^2}{E}k_R = 0 \qquad 3.115$$

Minimizing Equation 3.114 with respect to B_2 gives:

$$\frac{d\Pi}{dB_2} = \frac{E}{2L^3}\left(2B_2\left[I_z k_{RR} - \frac{N_x L^2}{E}k_R\right] + 2B_3 y_0 \,.\frac{N_x L^2}{E}k_R\right) = 0$$

That is:

$$B_2\left[I_z k_{RR} - \frac{N_x L^2}{E}k_R\right] + B_3 y_0 \,.\frac{N_x L^2}{E}k_R = 0 \qquad 3.116$$

Minimizing Equation 3.114 with respect to B_3 gives:

$$\frac{d\Pi}{dB_3} = \frac{E}{2L^3}\left(2B_3\left[I_\omega k_{RR} + \frac{L^2}{E}GJk_R - \frac{N_x L^2}{E}.\frac{I_0}{A}k_R\right] + 2B_2 y_0 \,.\frac{N_x L^2}{E}k_R - 2B_1 z_0 \,.\frac{N_x L^2}{E}k_R\right) = 0$$

That is:

$$B_3\left[I_\omega k_{RR} + \frac{L^2}{E}GJk_R - \frac{N_x L^2}{E}.\frac{I_0}{A}k_R\right] + B_2 y_0 \,.\frac{N_x L^2}{E}k_R - B_1 z_0 \,.\frac{N_x L^2}{E}k_R \;= 0 \qquad 3.117$$

Rearranging Equations 3.115 gives:

$$B_1\left[\frac{EI_y}{L^2}\frac{k_{RR}}{k_R} - N_x\right] - B_3 z_0 \,.N_x = 0 \qquad 3.118$$

Rearranging Equations 3.116 gives:

$$B_2\left[\frac{EI_z}{L^2}\frac{k_{RR}}{k_R} - N_x\right] + B_3 y_0 \,.N_x = 0 \qquad 3.119$$

Rearranging Equations 3.117 gives:

$$B_3\left[\frac{EI_\omega}{L^2}\frac{k_{RR}}{k_R} + GJ - N_x.\frac{I_0}{A}\right] + B_2 y_0 \,.N_x - B_1 z_0 \,.N_x \;= 0 \qquad 3.120$$

For pure flexural buckling case, the flexural critical buckling load is defined from Equations 3.118, 3.119 and 3.120 as:

$$\frac{N_c L^2}{EI} = \frac{k_{RR}}{k_R} \qquad 3.121$$

Where: I can be either I_y, I_z or I_ω as the case may be.

Rearranging Equation 3.121 gives:

$$N_c = \frac{EI}{L^2}.\frac{k_{RR}}{k_R} \qquad 3.122$$

Equation 3.122 is rewritten for various second moments of area as seen in Equation 3.118, 3.119 and 3.120:

$$N_{cy} = \frac{EI_y}{L^2}.\frac{k_{RR}}{k_R} \qquad 3.123$$

$$N_{cz} = \frac{EI_z}{L^2}.\frac{k_{RR}}{k_R} \qquad 3.124$$

$$N_{c\omega} = \frac{EI_\omega}{L^2}.\frac{k_{RR}}{k_R} \qquad 3.125$$

Substituting Equations 3.123, 3.124 and 3.125 into Equations 3.118, 3.119 and 3.120 respectively gives:

$$B_1\left[N_{cy} - N_x\right] - B_3 z_0\,.N_x = 0 \qquad 3.126$$

$$B_2[N_{cz} - N_x] + B_3 y_0\,.N_x = 0 \qquad 3.127$$

$$B_3\left[(N_{c\omega} + GJ) - N_x.\frac{I_0}{A}\right] + B_2 y_0\,.N_x - +B_1 z_0\,.N_x\ = 0 \qquad 3.128$$

Rewriting Equation 3.128 gives:

$$B_3[N_\emptyset - N_x.]\frac{I_0}{A} + B_2 y_0\,.N_x - B_1 z_0\,.N_x\ = 0 \qquad 3.129$$

Where:

$$N_\emptyset = (N_{c\omega} + GJ)\frac{A}{I_0} \qquad 3.130$$

$$N_{c\omega} = \frac{EI_\omega}{L^2}.\frac{k_{RR}}{k_R}; \qquad I_\omega = I_{yz} = I_y.{h_i}^2 + I_z.{b_i}^2 = warping\ constant$$

I_z is the second moment of area about (around) y axis and I_y is the second moment of area about (around) z axis.

Equations 3.126, 3.127 and 3.128 can be put in matrix forms as:

$$\begin{bmatrix} N_{cy} - N_x & 0 & -z_0 \,.\, N_x \\ 0 & N_{cz} - N_x & y_0 \,.\, N_x \\ -z_0 . N_x & y_0 . N_x & [N_\emptyset - N_x .] \dfrac{I_0}{A} \end{bmatrix} \begin{bmatrix} B_1 \\ B_2 \\ B_3 \end{bmatrix} = 0 \qquad 3.131$$

For non-trivial solution, the determinant of Equation 3.131 must be zero. That is:

$$\begin{vmatrix} N_{cy} - N_x & 0 & -z_0 \,.\, N_x \\ 0 & N_{cz} - N_x & y_0 \,.\, N_x \\ -z_0 . N_x & y_0 . N_x & [N_\emptyset - N_x .] \dfrac{I_0}{A} \end{vmatrix} = 0 \qquad 3.132$$

Equation 3.132 is rewritten as:

$$\begin{bmatrix} a_{11} & 0 & a_{13} \\ 0 & a_{22} & a_{23} \\ a_{31} & a_{32} & a_{33} \end{bmatrix} \begin{bmatrix} B_1 \\ B_2 \\ B_3 \end{bmatrix} = 0 \qquad 3.133$$

Where:

$$a_{11} = N_{cy} - N_x \qquad 3.134$$

$$a_{13} = -z_0 \,.\, N_x \qquad 3.135$$

$$a_{22} = N_{cz} - N_x \qquad 3.136$$

$$a_{23} = y_0 \,.\, N_x \qquad 3.137$$

$$a_{31} = -z_0 . N_x \qquad 3.138$$

$$a_{32} = y_0 . N_x \qquad 3.139$$

$$a_{33} = [N_\emptyset - N_x .] \frac{I_0}{A} \qquad 3.140$$

Solving Equation 3.133 gives:

$$a_{11} \begin{vmatrix} a_{22} & a_{23} \\ a_{32} & a_{33} \end{vmatrix} + a_{13} \begin{vmatrix} 0 & a_{22} \\ a_{31} & a_{32} \end{vmatrix} = 0 \qquad 3.141$$

Solving Equation 3.141 gives:

$$a_{11}[a_{22} . a_{33} - a_{23} . a_{32}] + a_{13}[0 . a_{32} - a_{22} . a_{31}] = 0 \qquad 3.142$$

Simplifying Equation 3.142 gives:

$$a_{11}a_{22}.a_{33} - a_{11}a_{23}.a_{32} - a_{13}.a_{22}.a_{31} = 0 \qquad 3.143$$

Substituting Equations 3.134 to 3.140 into Equation 3.143 gives:

$$\left(N_{cy} - N_x\right)(N_{cz} - N_x).\left([N_{\emptyset} - N_x.]\frac{I_0}{A}\right) - \left(N_{cy} - N_x\right)(y_0\,.N_x).(y_0.N_x)$$

$$-(-z_0\,.N_x).(N_{cz} - N_x).(-z_0.N_x) = 0 \qquad 3.144$$

Expanding Equation 3.144 gives:

$$-\frac{I_0}{A}{N_x}^3 + \frac{I_0}{A}{N_x}^2 N_{cy} + \frac{I_0}{A}{N_x}^2 N_{cz} - \frac{I_0}{A}N_x N_{cy} N_{cz} + \frac{I_0}{A}{N_x}^2 N_{\emptyset} - \frac{I_0}{A}N_x N_{cy} N_{\emptyset} - \frac{I_0}{A}N_x N_{cz} N_{\emptyset}$$

$$+\frac{I_0}{A}N_{cy} N_{cz} N_{\emptyset} - {y_0}^2.N_{cy}\,.{N_x}^2 + {y_0}^2\,.{N_x}^3 - N_{cz}{z_0}^2\,.{N_x}^2 + {z_0}^2\,.{N_x}^3 = 0$$

That is:

$$-\frac{I_0}{A}{N_x}^3 + {y_0}^2\,.{N_x}^3 + {z_0}^2\,.{N_x}^3 + \frac{I_0}{A}{N_x}^2 N_{cy} + \frac{I_0}{A}{N_x}^2 N_{cz} + \frac{I_0}{A}{N_x}^2 N_{\emptyset} - {y_0}^2.N_{cy}\,.{N_x}^2 - N_{cz}{z_0}^2\,.{N_x}^2$$

$$-\frac{I_0}{A}N_x N_{cy} N_{cz} - \frac{I_0}{A}N_x N_{cy} N_{\emptyset} - \frac{I_0}{A}N_x N_{cz} N_{\emptyset} + \frac{I_0}{A}N_{cy} N_{cz} N_{\emptyset} = 0$$

That is:

$$\left({y_0}^2 + {z_0}^2 - \frac{I_0}{A}\right).{N_x}^3 + \left(\frac{I_0}{A}\left[N_{cy} + N_{cz} + N_{\emptyset}\right] - {y_0}^2.N_{cy} - {z_0}^2.N_{cz}\right).{N_x}^2$$

$$-\left(\frac{I_0}{A}N_{cy} N_{cz} + \frac{I_0}{A}N_{cy} N_{\emptyset} + \frac{I_0}{A}N_{cz} N_{\emptyset}\right)N_x + \frac{I_0}{A}N_{cy} N_{cz} N_{\emptyset} = 0 \qquad 3.145$$

Multiplying Equation 3.145 by A/I_0 gives:

$$\left([{y_0}^2 + {z_0}^2]\frac{A}{I_0} - 1\right).{N_x}^3 + \left(N_{cy} + N_{cz} + N_{\emptyset} - \left[{y_0}^2.N_{cy} + {z_0}^2.N_{cz}\right]\frac{A}{I_0}\right).{N_x}^2$$

$$-\left(N_{cy} N_{cz} + N_{cy} N_{\emptyset} + N_{cz} N_{\emptyset}\right)N_x + N_{cy} N_{cz} N_{\emptyset} = 0 \qquad 3.146$$

Rearranging Equation 3.146 gives:

$$\left(1-[{y_0}^2+{z_0}^2]\frac{A}{I_0}\right).{N_x}^3+\left([{y_0}^2.N_{cy}+{z_0}^2.N_{cz}]\frac{A}{I_0}-[N_{cy}+N_{cz}+N_{\emptyset}]\right).{N_x}^2$$

$$+\left(N_{cy}N_{cz}+N_{cy}N_{\emptyset}+N_{cz}N_{\emptyset}\right)N_x-N_{cy}N_{cz}N_{\emptyset}=0 \qquad 3.147$$

Rewriting Equation 3.147 gives:

$$D_1.{N_x}^3+D_2.{N_x}^2+D_3.N_x+D_4=0 \qquad 3.148$$

Where:

$$D_1=1-[{y_0}^2+{z_0}^2]\frac{A}{I_0} \qquad 3.149$$

$$D_2=[{y_0}^2.N_{cy}+{z_0}^2.N_{cz}]\frac{A}{I_0}-N_{cy}-N_{cz}-N_{\emptyset} \qquad 3.150$$

$$D_3=N_{cy}N_{cz}+N_{cy}N_{\emptyset}+N_{cz}N_{\emptyset} \qquad 3.151$$

$$D_4=-N_{cy}N_{cz}N_{\emptyset} \qquad 3.152$$

3.3.1.1 Visual Basic Iterative Program for Determining the Roots of Polynomials In The Case of General Unsymmetrical Open Section

An iterative program is written in Visual Basic language to determine the roots of polynomials as the one presented on Equation 3.148.

The program is presented as:

```
Private Sub mnustart_Click()
N = InputBox("WHAT IS THE Degree of Polynomial"): N = N * 1
ReDimA(N, N), B(N, N), A1(N, N), B1(N, N), C(N, N), Eig(N)
ReDimD(N + 1), T(N + 1), L(N)
' ROOT OF THE CHARACTERISTIC EQUATION BEGINS HERE
For X = 1 To N + 1
D(X) = InputBox([X], "ENTER D"): D(X) = D(X) * 1
```

```
Next X
Z = N - 1: X = 2
Text1.Text = Text1.Text + CStr(D(1) & "L" & N)
For X = 2 To N
Text1.Text = Text1.Text + (" + "& D(X) & "L" & Z)
Z = Z - 1
Next X
Text1.Text = Text1.Text + (" + "& D(X))
Text1.Text = Text1.Text + (" ") &vbCrLf: Text1.Text = Text1.Text + (" ") &vbCrLf
Text1.Text = Text1.Text + (" ") &vbCrLf: Text1.Text = Text1.Text + (" ") &vbCrLf
For J = 1 To N + 1
Text1.Text = Text1.Text + ("    D(" & J & ") =" & D(J)) &vbCrLf
Next J
Text1.Text = Text1.Text + (" ") &vbCrLf: Text1.Text = Text1.Text + (" ") &vbCrLf
Text1.Text = Text1.Text + (" ") &vbCrLf: Text1.Text = Text1.Text + (" ") &vbCrLf
 F = 0: FP = 0: LL = -5: M = N: Z = 0: CC = 1
For X = 1 To N
For Y = 1 To N + 1
 F = F + D(Y) * LL ^ M
M = M - 1
Next Y
 If F < 0 Or Abs(F) < 0.001 Then FF = 0 Else FF = 1
 KH = FF
```

```
7000  If Z = 100 Then L(X) = L(X - 1): GoTo 9000
LL = LL + 0.1
For Y = 1 To N + 1
F = F + D(Y) * LL ^ M
M = M - 1
Next Y
Z = Z + 1
If F < 0 Or Abs(F) < 0.001 Then FF = 0 Else FF = 1
If Abs(F) < 0.001 Then GoTo 8000
M = N: F = 0: FP = 0
If FF = KH Then GoTo 7000
8000  L(X) = LL
9000
F = 0: FP = 0:  M = N: Z = 0:  LL = LL + 0.1
Next X
1000 Text1.Text = Text1.Text + ("    ") &vbCrLf: Text1.Text = Text1.Text + ("    ") &vbCrLf
Text1.Text = Text1.Text + ("    ") &vbCrLf: Text1.Text = Text1.Text + ("    ") &vbCrLf
 M = N: F = 0: FP = 0
 For J = 1 To N
For X = 1 To 30
For Y = 1 To N + 1
F = F + D(Y) * L(J) ^ M
If Y = N + 1 Then GoTo 20000
```

```
FP = FP + M * D(Y) * L(J) ^ (M - 1)
20000 M = M - 1
Next Y
If FP = 0 Then GoTo 30000
L(J) = L(J) - F / FP
30000 M = N: F = 0: FP = 0
Next X
M = N: F = 0: FP = 0
Text1.Text = Text1.Text + ("    R(" & J & ") =" & L(J)) &vbCrLf
    Next J
End Sub
```

This program only returns real roots. It does not return imaginary roots (complex number roots).

It displays the root as “R(i) = n”. Where: “R” is the root, “i” is the number (term) of the root and “n” is the value of the root.

These roots are the buckling loads, N_x.

3.3.2 Case of Single Symmetrical Open Section

In this case it is assumed that the axis of symmetry is y axis. Hence, $z_0 = 0$. Substituting for z_0 equals zero into Equation 3.132 gives:

$$\begin{vmatrix} N_{cy} - N_x & 0 & 0 \\ 0 & N_{cz} - N_x & y_0 \,.\, N_x \\ 0 & y_0 . N_x & [N_\emptyset - N_x .] \dfrac{I_0}{A} \end{vmatrix} = 0 \qquad 3.158$$

Equation 3.158 can be written as two independent equations as:

$$N_{cy} - N_x = 0 \qquad 3.159$$

$$\begin{vmatrix} N_{cz} - N_x & y_0 \,.\, N_x \\ y_0 \,.\, N_x & [N_\emptyset - N_x.]\dfrac{I_0}{A} \end{vmatrix} = 0 \qquad 3.160$$

The determinant of Equation 3.160 is:

$$\left[1 - {y_0}^2 \frac{A}{I_0}\right] {N_x}^2 - [N_{cz} + N_\emptyset]N_x + N_\emptyset N_{cz} = 0 \qquad 3.161$$

Equation 3.161 is rewritten as:

$$D_1 {N_x}^2 + D_2 N_x + D_3 = 0 \qquad 3.162$$

Where:

$$D_1 = 1 - {y_0}^2 \frac{A}{I_0} \qquad 3.163$$

$$D_2 = -[N_{cz} + N_\emptyset] \qquad 3.164$$

$$D_3 = N_\emptyset N_{cz} \qquad 3.165$$

Using formula for the roots of quadratic equation, it is obtained that:

$$N_x = \frac{-D_2 \pm \sqrt{{D_2}^2 - 4D_1 D_3}}{2D_1} \qquad 3.166$$

Substituting Equations 3.163, 3.164 and 3.165 into Equation 3.166 gives:

$$N_x = \frac{[N_{cz} + N_\emptyset] \pm \sqrt{{N_{cz}}^2 + 2N_{cz}.N_\emptyset + {N_\emptyset}^2 - 4N_\emptyset N_{cz} + 4{y_0}^2 \frac{A}{I_0} N_\emptyset N_{cz}}}{2\left(1 - {y_0}^2 \frac{A}{I_0}\right)}$$

That is:

$$N_x = \frac{[N_{cz} + N_\emptyset] \pm \sqrt{{N_{cz}}^2 + {N_\emptyset}^2 + 2N_\emptyset N_{cz}\left(2{y_0}^2 \frac{A}{I_0} - 1\right)}}{2\left(1 - {y_0}^2 \frac{A}{I_0}\right)} \qquad 3.167$$

Simplifying Equation 3.167 gives:

$$N_x = \frac{(N_{cz} + N_{\emptyset} \pm \propto)}{2\left(1 - {y_0}^2 \frac{A}{I_0}\right)} \qquad 3.168$$

Where:

$$\propto = \sqrt{{N_{cz}}^2 + {N_{\emptyset}}^2 + 2N_{\emptyset}N_{cz}\left(2{y_0}^2 \frac{A}{I_0} - 1\right)} \qquad 3.169$$

Alternatively, the program written earlier in section 3.3.1 can be employed to solve the quadratic equation presented on Equation 3.162.

3.3.3 Case of Double Symmetrical Open Section

In this case it is the axes of symmetry are y axis and z axis. Hence, $y_0 = 0$ and $z_0 = 0$. Substituting for $y_0 = 0$ and $z_0 = 0$ into Equation 3.132 gives:

$$\begin{vmatrix} N_{cy} - N_x & 0 & 0 \\ 0 & N_{cz} - N_x & 0 \\ 0 & 0 & [N_{\emptyset} - N_x.]\frac{I_0}{A} \end{vmatrix} = 0 \qquad 3.170$$

Equation 3.170 can be written as three independent equations as:

$$N_{cy} - N_x = 0 \qquad 3.171$$

$$N_{cz} - N_x = 0 \qquad 3.172$$

$$N_{\emptyset} - N_x = 0 \qquad 3.173$$

The least of N_x from Equations 3.171, 3.172 and 3.173 is the critical buckling load.

3.4 Numerical problems

The cross sections of column under consideration are as shown in Figure3.6.

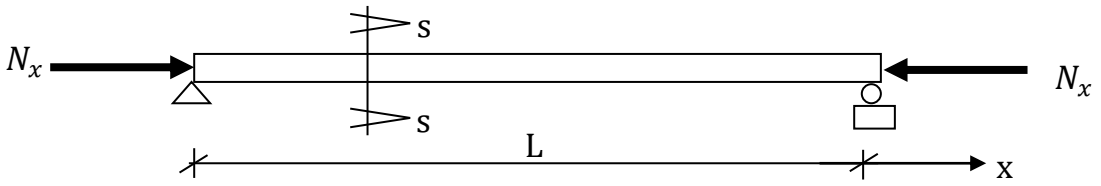

Figure 3.6a: Open cross section column under axial load

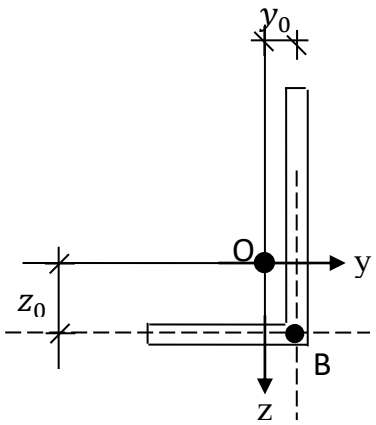

O is the centroid of section

B is the shear center of the section

Figure 3.6b: Section s-s (a general unsymmetrical open section)

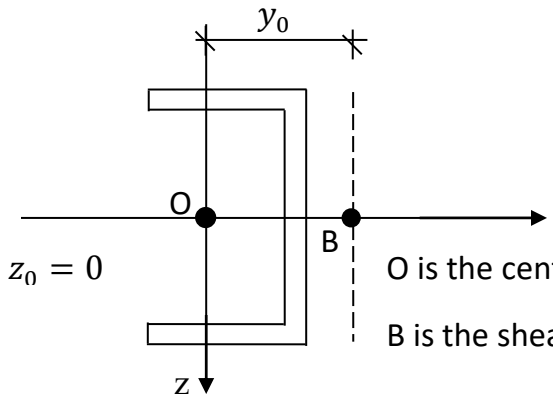

O is the centroid of section

B is the shear center of the section

Figure 3.6c: Section s-s (a single symmetrical open section), Symmetrical about y axis

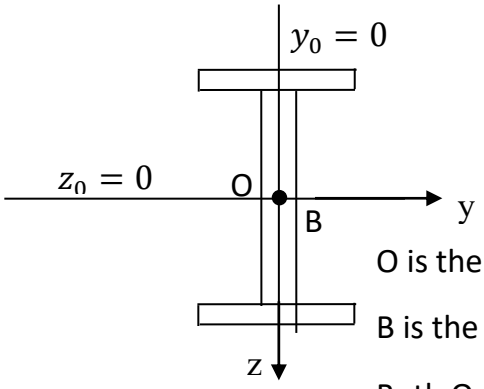

O is the centroid of section

B is the shear center of the section

Both O and B fall at the centroid

Figure 3.6d: Section s-s (a double symmetrical open section), symmetrical about both y axis and z axis

3.4.1 A Steel Unequal Angle with no Axis of Symmetry

The buckling of general unsymmetric unequal angle section with hinged ends as shown on Figure (3.6b) is the problem to be solved here. The requirements for the shape functions are that they must satisfy the geometric boundary conditions. The properties of the channel are tabulated as obtained from Steel Designer's Manual (7th Ed., 2012).

Section Designation is 200 x 150 x 12; Torsional index = X; Warping torsional constant = I_ω; St. Venant torsional constant = J.

D (mm)	B (mm)	t (mm)	M (kg/m)	A (cm^2)	I_z (cm^4)	I_y (cm^4)	I_ω (cm^6)	C_y (cm)	C_z (cm)
200	150	12	32	40.8	803	1650	494	6.08	3.61

For pinned ends at x = 0, x = L,

The ends of the column are free to warp and they can rotate about the x and y axes, but they cannot rotate about the z axis. The ends cannot deflect in the x and y directions also.

The geometric boundary conditions for this column are:

$v = 0 \quad (x = 0, L); w = 0 \quad (x = 0, L); \ \emptyset = 0 \quad (x = 0, L)$

The function that satisfies these boundary conditions is:

$v = B_1 \, Sin \, \pi R; \ w = B_1 \, Sin \, \pi R; \ \emptyset = B_1 \, Sin \, \pi R$

$D_1 \, . {N_x}^2 + D_2 N_x + D_3 = 0$

Where:

$D_1 \ = 1 - {y_0}^2 \frac{A}{I_0} \ ; \ D_2 \ = -[N_{cz} + N_\emptyset] \ ; \ D_3 \ = N_\emptyset N_{cz} \ ; N_\emptyset = \left(N_{cyz} + GJ\right) \frac{A}{I_0}$

For the given shape function:

$$k_{RR} = \int_0^1 \left[\frac{d^2h}{dR^2}\right]^2 dR = \pi^4 \int_0^1 Sin^2\, \pi R\, dR = \pi^4 \times \frac{1}{2} = \frac{\pi^4}{2}$$

$$k_R = \int_0^1 \left[\frac{dh}{dR}\right]^2 dR = \pi^2 \int_0^1 Cos^2\, \pi R\, dR = \pi^2 \times \frac{1}{2} = \frac{\pi^2}{2}$$

$$\frac{k_{RR}}{k_R} = \pi^2$$

Hence:

$$N_{cyz} = \pi^2 \frac{EI_\omega}{L^2};\ N_{cy} = \pi^2 \frac{EI_y}{L^2}\ ;\ N_{cz} = \pi^2 \frac{EI_z}{L^2}\ ;\ N_\emptyset = \left(\pi^2 \frac{EI_\omega}{L^2} + GJ\right)\frac{A}{I_0}$$

The warping torsional constant, $I_\omega$for an angle section, according to Bleich (1952) and Picard and Beaulieu (1991)is:

$$I_\omega = \frac{t^3}{36}(d'^3 + b'^3)$$

Where:

$$d' = d - \frac{t}{2} \quad and \quad b' = b - \frac{t}{2}$$

Therefore,

$$I_\omega = \frac{t^3}{36}\left(\left(200 - \frac{12}{2}\right)^3 + \left(150 - \frac{6}{2}\right)^3\right) = 493{,}793{,}664$$

That is:

$I_\omega = 493{,}793{,}664\text{mm}^6$

$I_z = 803\text{cm}^4 = 8{,}030{,}000\text{mm}^4$

$I_y = 1650\text{cm}^4 = 16{,}500{,}000\text{mm}^4$

$A = 40.8\text{cm}^2 = 4{,}080\text{mm}^2$

$y_0 = c_y = 6.08cm = 60.8mm$

$z_0 = c_z = 3.61cm = 36.1mm$

$I_0 = Ay_0{}^2 + Az_0{}^2 + I_y + I_z$

That is:

$I_0 = 4080mm^2 * (60.8mm)^2 + 4080mm^2 * (36.1mm)^2 + 16{,}500{,}000mm^4 + 8{,}030{,}000mm^4$

$= 44{,}929{,}388\ \text{mm}^4$

That is:

$I_0 = 44{,}929{,}388\ \text{mm}^4$

The St. Venant torsional constant, J for an angle section, according to Bleich (1952) and Picard and Beaulieu (1991) is:

$$J = \frac{t^3}{3}(d' + b')$$

$$J = \frac{12^3}{3}\left(\left(200 - \frac{12}{2}\right) + \left(150 - \frac{12}{2}\right)\right) = 194{,}688\text{mm}^4$$

The modulus of elasticity, E of steel is **210 GPa (**210, 000 N/mm^2)

The shear modulus (the coefficient of elasticity for a shearing or torsion force), G of steel is **77GPa (**77, 000 N/mm^2).

$$N_{cy} = \frac{EI_y}{L^2} \cdot \frac{k_{RR}}{k_R}$$

$$N_{cy} = \frac{210{,}000\ \text{N}/mm^2 \times 16{,}500{,}000\text{mm}^4}{(1000mm)^2} \times \pi^2 = 34{,}198{,}179.25\ \text{N}$$

$$N_{cz} = \frac{EI_z}{L^2} \cdot \frac{k_{RR}}{k_R}$$

$$N_{cz} = \frac{210{,}000\ \text{N}/mm^2 \times 8{,}030{,}000\text{mm}^4}{(1000mm)^2} \times \pi^2 = 16{,}643{,}113.90\ \text{N}$$

$$N_{c\omega} = \frac{EI_\omega}{L^2} \cdot \frac{k_{RR}}{k_R}$$

$$N_{c\omega} = \frac{210,000\ \text{N}/mm^2 \times 493{,}793{,}664\text{mm}^6}{(1000mm)^2} \times \pi^2 = 1{,}023{,}445{,}105.08\ \text{Nmm}^2$$

$$N_{\emptyset} = (N_{c\omega} + GJ)\frac{A}{I_0}$$

$$N_{\emptyset} = (1{,}023{,}445{,}105.08\ \text{Nmm}^2 + 77,000\ \text{N/mm}^2 \times 194{,}688\text{mm}^4) \times \frac{4{,}080\text{mm}^2}{44{,}929{,}388\ \text{mm}^4}$$

That is:

$$N_{\emptyset} = 1{,}454{,}256.13\ \text{N}$$

That is:

$$N_{\emptyset} = 1{,}454.26\ kN$$

$$D_1 = 1 - [{y_0}^2 + {z_0}^2]\frac{A}{I_0}$$

$$D_1 = 1 - [(60.8mm)^2 + (36.1mm)^2] \times \frac{4{,}080\text{mm}^2}{44{,}929{,}388\ \text{mm}^4} = 0.55$$

$$D_2 = \left[{y_0}^2.N_{cy} + {z_0}^2.N_{cz}\right]\frac{A}{I_0} - N_{cy} - N_{cz} - N_{\emptyset}$$

$$D_2 = [(60.8mm)^2 \times 34{,}198{,}179.25\text{N} + (36.1mm)^2 \times 16{,}643{,}113.90\ \text{N}] \times \frac{4{,}080\text{mm}^2}{44{,}929{,}388\ \text{mm}^4}$$

$$- 34{,}198{,}179.25\text{N} - 16{,}643{,}113.90\ \text{N} - 1{,}454{,}256.13\text{N}$$

$$D_2 = [3696.64\text{mm}^2 \times 34{,}198{,}179.25\text{N} + 1303.21\text{mm}^2 \times 16{,}643{,}113.90\ \text{N}] \times \frac{4{,}080\text{mm}^2}{44{,}929{,}388\ \text{mm}^4}$$

$$- 34{,}198{,}179.25\text{N} - 16{,}643{,}113.90\ \text{N} - 1{,}454{,}256.13\ \text{N}$$

$$D_2 = -38{,}846{,}001.64\ N$$

$$D_2 = -38{,}846.001\ \text{k}N$$

$$D_3 = N_{cy}N_{cz} + N_{cy}N_{\emptyset} + N_{cz}N_{\emptyset}$$

$$D_3 = 34{,}198{,}179.25\text{N} \times 16{,}643{,}113.90\ \text{N} + 34{,}198{,}179.25\text{N} \times 1{,}454{,}256.13\ \text{N} + 16{,}643{,}113.90\ \text{N} \times 1{,}454{,}256.13\ \text{N}$$

$$D_3 = 643{,}100{,}454{,}920{,}246.00\text{N}^2$$

$$D_3 = 643{,}100{,}454.920\text{kN}^2$$

$$D_4 = -N_{cy}N_{cz}N_{\emptyset}$$

$$D_4 = -34{,}198{,}179.25\text{N} \times 16{,}643{,}113.90\ \text{N} \times 1{,}454{,}256.13\ \text{N}$$

$$D_4 = -827{,}710{,}518{,}330{,}083{,}000{,}000.00\text{N}^3$$

$$D_4 = -827{,}710{,}518{,}330.083\text{kN}^3$$

$$D_1.{N_x}^3 + D_2.{N_x}^2 + D_3.N_x + D_4 = 0$$

$$0.55{N_x}^3 + -38{,}846.001\ \text{k}N \times {N_x}^2 + 643{,}100{,}454.920\text{kN}^2 \times N_x 930 - 827{,}710{,}518{,}330.083\text{kN}^3 = 0$$

$${N_x}^3 - 70{,}629.09\text{k}N.{N_x}^2 + 1{,}169{,}273{,}554\text{kN}^2.N_x - 1{,}504{,}930{,}000{,}000\text{kN}^3 = 0$$

Solving for the roots of this cubic equation gave only one real root as 1403.72kN

3.4.2 A Steel Channel With Only One Axis of Symmetry

The buckling of single symmetric channel section with hinged ends as shown on Figure (3.6c) is the problem to be solved here. The requirements for the shape functions are that they must satisfy the geometric boundary conditions. The properties of the channel are tabulated as obtained from Steel Designer's Manual (7th Ed., 2012).

Section Designation is 180 x 75 x 20 Channel

d (mm)	b (mm)	t_w(mm)	t_f (mm)	A (cm^2)	I_z (cm^4)	I_y (cm^4)	y_0 (cm)	z_0 (cm)
180	75	6.0	10.5	25.9	1370	146	2.87	0

For pinned ends at x = 0, x = L,

The geometric boundary conditions for this column are:

$v = 0 \;\; (x = 0, L); w = 0 \;\; (x = 0, L); \; \emptyset = 0 \;\; (x = 0, L)$

The function that satisfies these boundary conditions are:

$v = B_1 \, Sin \, \pi R; \; w = B_1 \, Sin \, \pi R; \; \emptyset = B_1 \, Sin \, \pi R$

$D_1 \, . {N_x}^2 + D_2 N_x + D_3 = 0$

Where:

$D_1 \; = 1 - {y_0}^2 \frac{A}{I_0}$

$D_2 \; = -[N_{cz} + N_\emptyset]$

$D_3 \; = N_\emptyset N_{cz} \, ; N_\emptyset = \left(N_{cyz} + GJ\right) \frac{A}{I_0}$

For the given shape function:

$$k_{RR} = \int_0^1 \left[\frac{d^2h}{dR^2}\right]^2 dR = \pi^4 \int_0^1 Sin^2 \, \pi R \, dR = \pi^4 \times \frac{1}{2} = \frac{\pi^4}{2}$$

$$k_R = \int_0^1 \left[\frac{dh}{dR}\right]^2 dR = \pi^2 \int_0^1 Cos^2 \, \pi R \, dR = \pi^2 \times \frac{1}{2} = \frac{\pi^2}{2}$$

$$\frac{k_{RR}}{k_R} = \pi^2$$

$y_0 = 2.87cm = 28.7mm$

$z_0 = 0cm = 0mm$

$I_z = 1370\text{cm}^4 = 13{,}700{,}000\text{mm}^4$

$I_y = 146\text{cm}^4 = 1{,}460{,}000\text{mm}^4$

$A = 25.9\text{cm}^2 = 2{,}590\text{mm}^2$

$I_0 = Ay_0{}^2 + Az_0{}^2 + I_y + I_z$

$I_0 = 25.9\text{cm}^2 \times (2.87cm)^2 + 25.9\text{cm}^2 \times (0cm)^2 + 1370cm^4 + 146cm^4$

$= 1729.336\ cm^4 = 17{,}293{,}360\ mm^4$

The warping torsional constant is given by Galambos (1968) and SSRC(1998) in separate works as:

$$I_\omega = d'^2 b'^3 t_f \left[\frac{1-3\alpha}{6} + \frac{\alpha^2}{2}\left(1 + \frac{d't_w}{6b't_f}\right)\right] = 7{,}269{,}217{,}776.70\text{mm}^6$$

The St. Venant torsional constant for a channel cross section is given by SSRC (1998) as:

$$J = \frac{1}{3}\left(2b't_f^3 + d't_w^3\right) = 67{,}770mm^4$$

The modulus of elasticity, E of steel is 210 GPa (210, 000 N/mm2)

The shear modulus (the coefficient of elasticity for a shearing or torsion force), G of steel is 77GPa (77, 000 N/mm2)

$$N_{c\omega} = \pi^2 \frac{EI_\omega}{L^2} = \pi^2 \times \frac{210{,}000\ \text{N}/mm^2 \times 7{,}269{,}217{,}776.70\text{mm}^6}{(1000mm)^2} = 15{,}066{,}303{,}789.89\text{Nmm}^2$$

That is:

$N_{c\omega} = 15{,}066.30\ \text{Nm}^2 = 15.07\ \text{kNm}^2$

$$N_{cy} = \pi^2 \frac{EI_y}{L^2} = \pi^2 \times \frac{210{,}000\ \text{N}/mm^2 \times 1{,}460{,}000\text{mm}^4}{(1000mm)^2} = 3{,}026{,}020.71\text{N}$$

That is:

$N_{cy} = 3{,}026.02$ kN

$$N_{cz} = \pi^2 \frac{EI_z}{L^2} = \pi^2 \times \frac{210,000\ \text{N}/mm^2 \times 13{,}700{,}000\text{mm}^4}{(1000mm)^2} = 28{,}394{,}851.86\text{N}$$

That is:

$N_{cz} = 28{,}394.85$ kN

$$N_{\emptyset} = \left(\pi^2 \frac{EI_{\omega}}{L^2} + GJ\right)\frac{A}{I_0}$$

$$N_{\emptyset} = \left(\pi^2 \times \frac{210,000\ \text{N}/mm^2 \times 7{,}269{,}217{,}776.70\text{mm}^6}{(1000mm)^2} + 77,000\ \text{N}/mm^2 \times 67{,}770\text{mm}^4\right) \times \frac{2{,}590\text{mm}^2}{17{,}293{,}360\ \text{mm}^4}$$

$= 3{,}037{,}993{,}005.76N$

That is:

$N_{\emptyset} = 3{,}037{,}993.01kN$

$$D_1 = 1 - {y_0}^2 \frac{A}{I_0} = 1 - (2.87cm)^2 \frac{25.9\text{cm}^2}{1729.336\ cm^4} = 0.876637192$$

$$D_2 = -[N_{cz} + N_{\emptyset}] = -[28{,}394.85\ \text{kN} + 3{,}037{,}993.01kN] = -3{,}066{,}387.86\ \text{kN}$$

$$D_3 = N_{\emptyset}N_{cz} = 3{,}037{,}993.01kN \times 28{,}394.85\ \text{kN} = 86{,}263{,}361{,}356.01\text{kN}^2$$

$D_1 . {N_x}^2 + D_2N_x + D_3 = 0$

$D_1 . {N_x}^2 + D_2N_x + D_3 = 0$

$$N_x = \frac{-D_2 \pm \sqrt{{D_2}^2 - 4D_1D_3}}{2D_1}$$

$4D_1D_3 = 4 \times 0.876637192 \times 86{,}263{,}361{,}356.01\text{kN}^2 = 302{,}486{,}683{,}318.89\text{kN}^2$

302,486,683,318.89

$$N_x = \frac{3{,}066{,}387.86\ \text{kN} \pm \sqrt{(3{,}066{,}387.86\ \text{kN})^2 - 302{,}486{,}683{,}318.89\text{kN}^2}}{2 \times 0.876637192}$$

$N_{x1} = 3{,}469{,}536.55\ \text{kN}$

$N_{x2} = 28{,}361.88\ \text{kN}$

For a section of single symmetry, the lesser of N_{cy}, N_{x1} and N_{x2} is the critical buckling load. In this case, N_{cy} is lesser. Thus, the critical buckling load is:

$$N_{cy} = 3{,}026.02\ \text{kN}$$

3.4.3 A Steel Stanchion With Double Axes of Symmetry

Buckling of double symmetrical H-section with hinged ends of open cross section (L=1) in Figure (3.6b). The requirements for the shape functions are that they must satisfy the geometric boundary conditions. The properties of the channel are tabulated as obtained from Steel Designer's Manual (Seventh Edition).

Section Designation = 203 x 203x46 universal column

d (mm)	b (mm)	t_w(mm)	t_f (mm)	A (cm^2)	I_z (cm^4)	I_y (cm^4)	y_0 (cm)	z_0 (cm)
203.2	203.6	7.2	11	58.7	1550	4570	0	0

For pinned ends at x = 0, x = L,

The geometric boundary conditions for this column are:

$v = 0 \quad (x = 0, L); w = 0 \quad (x = 0, L); \ \emptyset = 0 \quad (x = 0, L)$

The function that satisfies these boundary conditions are:

$v = B_1 \, Sin \, \pi R; \ w = B_1 \, Sin \, \pi R; \ \emptyset = B_1 \, Sin \, \pi R$

For the given shape function:

$$k_{RR} = \int_0^1 \left[\frac{d^2h}{dR^2}\right]^2 dR = \pi^4 \int_0^1 Sin^2\,\pi R\,dR = \pi^4 \times \frac{1}{2} = \frac{\pi^4}{2}$$

$$k_R = \int_0^1 \left[\frac{dh}{dR}\right]^2 dR = \pi^2 \int_0^1 Cos^2\,\pi R\,dR = \pi^2 \times \frac{1}{2} = \frac{\pi^2}{2}$$

$$\frac{k_{RR}}{k_R} = \pi^2$$

$y_0 = 0\,mm$

$z_0 = 0\,mm$

$A = 58.7\text{cm}^2 = 5{,}870\text{mm}^2$

$I_z = 1550\text{cm}^4 = 15{,}500{,}000\text{mm}^4$

$I_y = 4570\text{cm}^4 = 45{,}700{,}000\text{mm}^4$

$I_0 = Ay_0{}^2 + Az_0{}^2 + I_y + I_z$

$I_0 = 58.7\text{cm}^2 \times (0cm)^2 + 58.7\text{cm}^2 \times (0cm)^2 + 45{,}700{,}000\text{mm}^4 + 15{,}500{,}000\text{mm}^4$

$= 61{,}200{,}000.00mm^4$

The formula for calculating the warping torsional constant, $I_\omega$for an I-section or H-section is given by Galambos(1968), Picard and Beaulieu (1991) in their separate works as:

$$I_\omega = \frac{1}{24}\left(d'^2 b^3 t_f\right) = 142{,}896{,}480{,}083.35\text{mm}^6$$

The formula for calculating the St. Venant torsional constant, J for an I-section or H-section is given by St. Venant torsional constant, J for an I-sectionis given by Galambos(1968) as:

$$J = \frac{1}{3}\left(2bt_f^3 + d't_w^3\right) = 204{,}573.82\text{mm}^4$$

The modulus of elasticity, E of steel is **210 GPa (**210, 000 N/mm^2)

The shear modulus (the coefficient of elasticity for a shearing or torsion force), G of steel is **77GPa (**77, 000 N/mm^2)

$$N_{cy} = \frac{EI_y}{L^2}.\frac{k_{RR}}{k_R} = \pi^2 \times \frac{210,000\ \text{N}/mm^2 \times 45{,}700{,}000\text{mm}^4}{(1000mm)^2} = 94{,}718{,}590\ N = 94{,}718.59\ \text{kN}$$

That is:

$$N_{cy} = 94{,}718.59\ kN$$

$$N_{cz} = \frac{EI_z}{L^2}.\frac{k_{RR}}{k_R} = \pi^2 \times \frac{210,000\ \text{N}/mm^2 \times 15{,}500{,}000\text{mm}^4}{(1000mm)^2} = 32{,}125{,}560N = 32{,}125.56\ \text{kN}$$

That is:

$$N_{cz} = 32{,}125.56\ \text{kN}$$

$$N_{c\omega} = \frac{EI_\omega}{L^2}.\frac{k_{RR}}{k_R} = \pi^2 \times \frac{210,000\ \text{N}/mm^2 \times 142{,}896{,}480{,}083.35\text{mm}^6}{(1000mm)^2}$$

$$= 296{,}169{,}663{,}024.38Nmm^2$$

That is:

$$N_{c\omega} = 296{,}169{,}663.024\text{k}Nmm^2$$

$$N_\emptyset = (N_{c\omega} + GJ)\frac{A}{I_0}$$

$$N_\emptyset = (296{,}169{,}663{,}024.38Nmm^2 + 77,000\ \text{N}/mm^2 \times 204{,}573.82\text{mm}^4) \times \frac{5{,}870\text{mm}^2}{61{,}200{,}000.00mm^4}$$

$$= 29{,}917{,}990\ \text{N} = 29{,}917.99\ \text{kN}$$

That is:

$$N_\emptyset = 29{,}917.99\ \text{kN}$$

$$N_{cy} = 94{,}718.59\ kN;\ N_{cz} = 32{,}125.56\ \text{kN};\ N_\emptyset = 29{,}917.99\ \text{kN}$$

The least of N_{cz}, N_{cy} and N_ϕ gives the critical buckling load. That is:

$$N_x = 29{,}917.99\ \text{kN}$$

CHAPTER 4

RESULTS AND DISCUSSIONS

4.1 Presentation of results

The results obtained in this study are presented in this chapter.

4.1.1 Total Potential Energy Functional for Thin-Wall Column of Open Cross-Sectionin

Total potential energy functional of thin-walled column for flexural buckling

$$\Pi = \frac{EI_z}{2}\int\left(\frac{d^2w}{dx^2}\right)^2 dx + \frac{EI_y}{2}\int\left(\frac{d^2v}{dx^2}\right)^2 dx - \frac{N_x}{2}\int_0^L\left(\frac{dw}{dx}\right)^2 dx - \frac{N_x}{2}\int_0^L\left(\frac{dv}{dx}\right)^2 dx \qquad 4.1$$

Total potential energy functional of thin-walled column for torsional buckling where the ends is free to warp

$$\Pi = \frac{EI_\omega}{2}\int\left(\frac{d^2\phi}{dx^2}\right)^2 dx - \frac{N}{2}\frac{\mathrm{I_0}}{\mathrm{A_c}}\int_0^L\left(\frac{d\phi}{dx}\right)^2 dx \qquad 4.2$$

Total potential energy functional of thin-walled column for torsional buckling where the ends are prevented from warping

$$\Pi = \frac{EI_\omega}{2}\int\left(\frac{d^2\phi}{dx^2}\right)^2 dx - \frac{N_x}{2}\frac{\mathrm{I_0}}{\mathrm{A_c}}\int_0^L\left(\frac{d\phi}{dx}\right)^2 dx + \frac{GJ}{2}\int\left(\frac{d\phi}{dx}\right)^2 dx \qquad 4.3$$

Total potential energy functional of thin-walled column for torsional-flexural buckling

$$\Pi = \frac{E}{2L^3}\int\left[I_z\left(\frac{d^2w}{dR^2}\right)^2 + I_y\left(\frac{d^2v}{dR^2}\right)^2 + I_\omega\left(\frac{d^2\phi}{dR^2}\right)^2 + \frac{GJL^2}{E}\left(\frac{d\phi}{dR}\right)^2 - \frac{N_xL^2}{E}\left(\frac{dv}{dR}\right)^2 - \frac{N_xL^2}{E}\left(\frac{dw}{dR}\right)^2 - \frac{N_xI_0L^2}{EA}\cdot\left(\frac{d\emptyset}{dR}\right)^2 + \frac{2y_0N_xL^2}{E}\cdot\frac{dw}{dR}\cdot\frac{d\emptyset}{dR} - \frac{2z_0N_xL^2}{E}\cdot\frac{dv}{dR}\cdot\frac{d\emptyset}{dR}\right] dR \qquad 4.4$$

4.1.2 Governing differential equations

The general governing Equation of the thin-walled open cross section column undergoing torsional-flexural buckling as derived in this work is presented as:

$$\frac{d^4w}{dR^4} + \frac{d^2w}{dR^2}.\frac{N_T L^2}{EI_T} = 0 \qquad 4.5$$

4.1.3 Flexural critical buckling load

The general flexural critical buckling load equations derived in this work is presented as:

$$N_c = \frac{EI}{L^2}.\frac{k_{RR}}{k_R} \qquad 4.6$$

The flexural critical buckling load derived in this work for various second moments of area are

$$N_{cy} = \frac{EI_y}{L^2}.\frac{k_{RR}}{k_R} \qquad 4.7$$

$$N_{cz} = \frac{EI_z}{L^2}.\frac{k_{RR}}{k_R} \qquad 4.8$$

$$N_{c\omega} = \frac{EI_\omega}{L^2}.\frac{k_{RR}}{k_R} \qquad 4.9$$

$$I_\omega = I_{yz} = I_y.{h_i}^2 + I_z.{b_i}^2 = warping\ constant \qquad 4.10$$

I_z is the second moment of area about (around) y axis and I_y is the second moment of area about (around) z axis

4.1.4 Buckling load formula for unsymmetrical open section of thin-walled column

The buckling load formula for unsymmetrical open thin-walled column section derived in this work is presented as:

$$D_1.{N_x}^3 + D_2.{N_x}^2 + D_3.N_x + D_4 = 0 \qquad 4.11$$

Where:

$$D_1 = 1 - [{y_0}^2 + {z_0}^2]\frac{A}{I_0} \quad 4.12$$

$$D_2 = \left[{y_0}^2.N_{cy} + {z_0}^2.N_{cz}\right]\frac{A}{I_0} - N_{cy} - N_{cz} - N_{\emptyset} \quad 4.13$$

$$D_3 = N_{cy}N_{cz} + N_{cy}N_{\emptyset} + N_{cz}N_{\emptyset} \quad 4.14$$

$$D_4 = -N_{cy}N_{cz}N_{\emptyset} \quad 4.15$$

4.1.5 Buckling load formula for single symmetrical open section of thin-walled column

The buckling load formula for single symmetrical is presented as:

$$N_x = \frac{(N_{cz} + N_{\emptyset} \pm \propto)}{2\left(1 - {y_0}^2\frac{A}{I_0}\right)} \quad 4.16$$

Where:

$$\propto = \sqrt{{N_{cz}}^2 + {N_{\emptyset}}^2 + 2N_{\emptyset}N_{cz}\left(2{y_0}^2\frac{A}{I_0} - 1\right)} \quad 4.17$$

$$N_{\emptyset} = (N_{c\omega} + GJ)\frac{A}{I_0}$$

4.1.6 Buckling load formula for double symmetrical open section of thin-walled column

The buckling load formula for double symmetrical are presented as:

$$N_{cy} - N_x = 0 \quad 4.18$$

$$N_{cz} - N_x = 0 \quad 4.19$$

$$N_{\emptyset} - N_x = 0 \quad 4.20$$

The least of N_x from Equations 4.18, 4.19 and 4.20 is the critical buckling load.

4.1.7 Results from numerical example

4.1.7.1 General unsymmetric unequal angle section

The results of numerical analysis for example case 1 is presented on tables 4.1 and Figure 4.1

Table 4.1 Critical buckling load of general unsymmetric unequal angle section with hinged ends

L (m)	$N_{x\,(KN)}$
1	1454.256134
1.25	1420.798386
1.5	1402.623806
1.75	1391.665108
2	1384.552491
2.25	1379.676105
2.5	1376.188054
2.75	1373.607291
3	1371.644409
3.25	1370.116826
3.5	1358.621543
3.75	1183.510322
4	1040.194619
4.25	921.4180707
4.5	821.882168
4.75	737.6449375
5	665.7245561

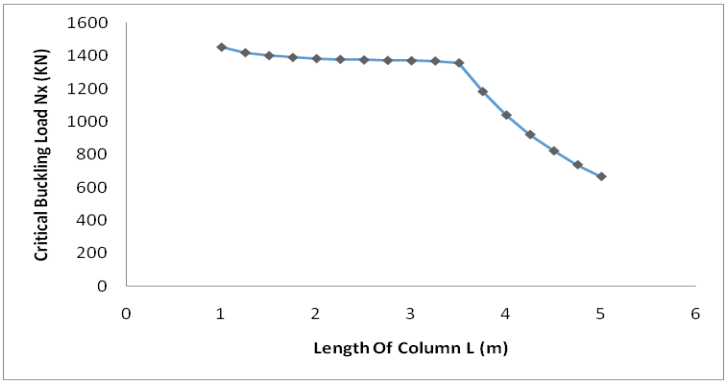

Figure 4.1: Graph of Critical buckling against the length of column for general unsymmetric unequal angle section.

4.1.7.2 Single symmetric channel section

The results of numerical analysis for example case 2 are presented on Tables 4.2 and Figure 4.2

Table 4.2 Critical buckling load of single symmetric channel section with hinged ends

L (m)	$N_{x\,(KN)}$
1	3026.02
1.25	1936.65
1.5	1344.9
1.75	988.09
2	756.51
2.25	597.73
2.5	484.16
2.75	400.13
3	336.22
3.25	286.49
3.5	247.02
3.75	215.18
4	189.13
4.25	167.53
4.5	149.43
4.75	134.12
5	121.04

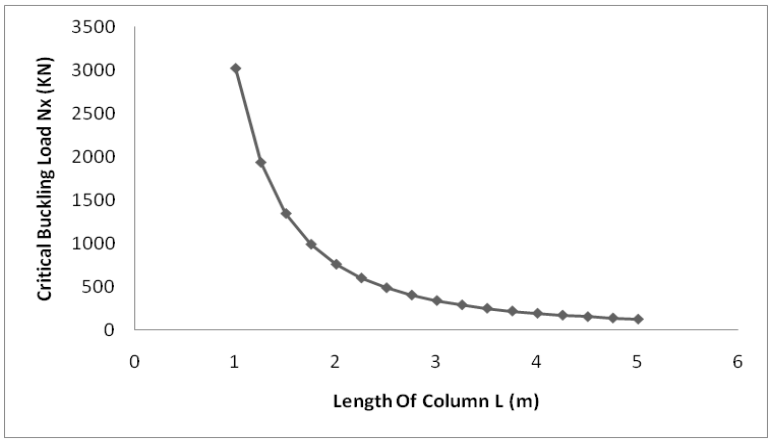

Figure 4.2: Graph of Critical buckling against the length of column for single symmetric channel section

4.1.7.3 Double symmetrical section

The results of numerical analysis for example case 3 are presented on Tables 4.3 and Figure 4.3

Table 4.3 Critical buckling load of double symmetrical section with hinged ends

L (m)	$N_{x\,(KN)}$
1	29917.99
1.25	19691.43
1.5	14136.26
1.75	10489.98
2	8031.39
2.25	6345.79
2.5	5140.09
2.75	4248.01
3	3569.51
3.25	3041.47
3.5	2622.49
3.75	2284.48
4	2007.85
4.25	1778.58
4.5	1586.45
4.75	1423.85
5	1285.02

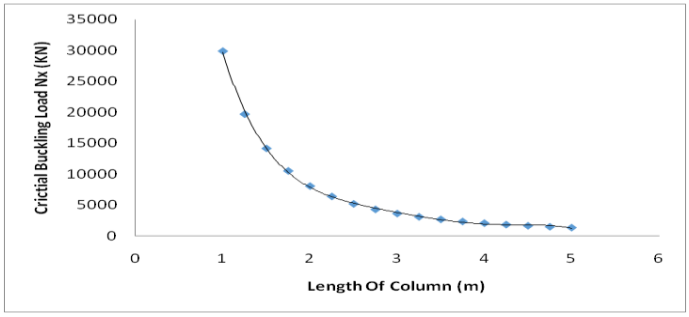

Figure 4.3: Graph of Critical buckling against the length of column for double symmetrical section

4.1.7.4 Comparison of Results with those of Jerath (2020)

The results obtained in this present study are compared with other existing theories to determine its efficacy. The results of Example case 1 to 3 are compared with the results obtained from Jerath (2020. The percentagedifference in results obtained in this study with respect to the corresponding results obtained by the other theories is calculated as follows:

$$Difference = \frac{\text{value obtained using present study} - \text{value obtained using model under comparison}}{\text{value obtained using model under comparison}} x100\%$$

Table 4.4 Comparison of critical buckling load for general unsymmetric unequal angle section with hinged ends

L (m)	Nx (kN) Present Study	Nx (kN) Jerath	% diff.
1.00	1454.256134	1462.53	+0.57%
1.25	1420.798386	1412.59	-0.58%
1.50	1402.623806	1394.21	-0.60%
1.75	1391.665108	1403.50	+0.85%
2.00	1384.552491	1391.18	+0.48%
2.25	1379.676105	1365.88	-1.00%
2.50	1376.188054	1362.34	-1.00%
2.75	1373.607291	1366.87	-0.49%
3.00	1371.644409	1375.79	+0.30%
3.25	1370.116826	1383.82	+1.00%
3.50	1358.621543	1345.03	-1.00%
3.75	1183.510322	1175.89	-0.64%
4.00	1040.194619	1048.18	+0.77%
4.25	921.4180707	912.21	-1.00%
4.50	821.882168	829.10	+0.88%
4.75	737.6449375	730.27	-1.00%
5.00	665.7245561	658.07	-1.15%

Table 4.5 Comparison of critical buckling load for single symmetric channel section with hinged ends

L (m)	Nx (kN) Present Study	Nx (kN) Jerath	% diff.
1	3026.02	3005.83	0.67
1.25	1936.65	1920.00	0.86
1.5	1344.90	1355.00	-0.75
1.75	988.09	980.00	0.82
2	756.51	749.00	0.99
2.25	597.73	592.00	0.96
2.5	484.16	480.00	0.86
2.75	400.13	396.00	1.03
3	336.22	333.00	0.96
3.25	286.49	284.00	0.87
3.5	247.02	249.00	-0.80
3.75	215.18	213.00	1.01
4	189.13	191.00	-0.99
4.25	167.53	166.00	0.91
4.5	149.43	150.80	-0.92
4.75	134.12	133.00	0.84
5	121.04	120.00	0.86

Table 4.6 Comparison of critical buckling load for double symmetrical section with hinged ends

L (m)	Nx (kN) Present Study	Nx (kN) Jerath	% diff.
1	29917.99	29750.00	0.56
1.25	19691.43	19800.00	-0.55
1.5	14136.26	14020.00	0.82
1.75	10489.98	10580.00	-0.86
2	8031.39	7960.00	0.89
2.25	6345.79	6290.00	0.88
2.5	5140.09	5185.00	-0.87
2.75	4248.01	4285.00	-0.87
3	3569.51	3530.00	1.11
3.25	3041.47	3010.00	1.04
3.5	2622.49	2645.00	-0.86
3.75	2284.48	2305.00	-0.90
4	2007.85	1989.00	0.94
4.25	1778.58	1755.00	1.33
4.5	1586.45	1600.00	-0.85
4.75	1423.83	1435.00	-0.78
5	1285.02	1270.00	1.17

4.2 Discussion of Results

The results of the numerical examples carried out in Chapter three were presented. In general, the equations were found to be reduced to a system of algebraic eigenvalue eigenvector problem. The buckling equations were found for single symmetric, double symmetric and general asymmetric column sections. The buckling modes were found as flexural torsional buckling modes. For single symmetric sections, it was found that the buckling behavior is described by a system of three homogeneous differential equations, two of which are uncoupled. If the thin-walled column in this case is hinged at both ends $z = 0$ and $z = l$, the solution of the one uncoupled buckling equation gives the expression for the critical buckling load in the direction of the axis of symmetry. For general asymmetric sectioned column the buckling mode was found to be a cubic polynomial. In the case of double symmetric sections, it was found that the buckling modes are uncoupled and double symmetric columns could fail by pure flexural buckling about the axes of symmetry or pure torsional buckling.

Generally, from Figures 4.1 to 4.2, the critical buckling loads decreased as the length of the column increased.

The results obtained in this present study are compared with other existing research to determine their efficacy. The results of Example cases 1 to 3 were compared with the corresponding solutions of the same problem presented by Jerath (2020) using differential equations method. The results were found to be the same.

The result was further compared with the solution obtained by Iyengar (1988 solution, which utilized the equilibrium of the deformed shape approach. Both solutions were found to be the same.

CHAPTER FIVE

CONCLUSION AND RECOMMENDATIONS

5.1 Conclusion

The research has introduced a clear and uncomplicated method for determining the critical buckling load of thin-walled columns with open cross-sections. The specific objectives outlined at the outset have been systematically addressed and achieved through analysis and computational methods.

Firstly, the total potential energy functional of a thin-walled column undergoing torsional-flexural buckling was derived. This foundational step provided the basis for formulating the governing equations that describe the stability conditions of such columns under combined bending and torsional loads.

Secondly, the differential equation governing the torsional-flexural buckling behavior of thin-walled columns with open cross-sections was derived. This equation encapsulates the complex interplay between bending and torsion, crucial for predicting critical buckling loads and modes.

Thirdly, an elastic buckling equation using energy formulation was derived. This equation provides a direct means to determine the critical buckling load of thin-walled columns, essential for structural design and assessment.

Fourthly, numerical methods were employed to solve practical problems related to torsional-flexural buckling. The developed methods were validated through comparisons with established theoretical results, demonstrating their accuracy and reliability in predicting buckling behavior under various loading conditions.

Finally, a Visual Basic program was developed to facilitate the practical application of the theoretical formulations. This program allows engineers and researchers to efficiently analyze and design thin-walled columns with open cross-sections, considering torsional-flexural buckling effects.

5.2 Recommendations

This work has demonstrated how to obtain the critical buckling load of thin-walled column of open sections.

This method will be a very useful method in the analysis of torsional-flexural buckling of thin-walled column of open cross section subjected to compressive loading. It is recommended that

1. this method be applied to the solution of thin-walled column of open cross section as it will reduce the complexity involved in the analysis of such column.

2. The method could be further explored by using it to obtain the critical buckling load of a prismatic column under a concentrated load.

3. Also, with the simplicity of this method it is recommended that this method be followed in the analysis of column of any boundary condition.

5.3 Contributions to knowledge

This work has made great strides in the analysis of thin-walled column of open cross section, contributing immensely to the body of knowledge in the analysis of thin-walled column. The following are the contributions to knowledge by this work:

1. It has provided a simple approach to obtaining the buckling load of a hinged thin-walled column of open cross section
2. It has provided a simple analytical method for the analysis of thin-walled column which lends itself to simple mathematical computations, making it very easy to use for both manual computation and also in computer aided computation.

References

Andreassen, M. J. (2012). *Distortional mechanics of thin-wall structural elements* (Doctoral dissertation). Department of Civil Engineering, Technical University of Denmark.

Anderson, J. M., & Trahair, N. S. (1972). Stability of monosymmetric beams and cantilevers. *Journal of the Structural Division, ASCE, 98*(1), 269-285.

Assadi, M., & Roeder, C. W. (1985). Stability of continuously restrained cantilevers. *Journal of Engineering Mechanics, 111*(12), 1440-1456.

Barsoum, R. S., & Gallagher, R. H. (1970). Finite element analysis of torsional and torsional-flexural stability problems. *International Journal for Numerical Method in Engineering, 2*(3), 335-352.

Bazeos, N., & Xykis, C. (2002). Elastic buckling analysis of 3-D trusses and frames with thin-walled members. *Computational Mechanics, 29*(6), 459-470.

Baird, D., Hendy, C., Wong, P., Jones, R., Sollis, A., & Nuttall, H. (2011). Design of the Olympic Park bridges H01 and L01. *IABSE Structural Engineering International*, February.

Bebiano, R., Silvestre, N., & Camotim, D. (2008). GBTUL – A code for the buckling analysis of cold formed steel members. In R. LaBoube & W.-W. Yu (Eds.), *Proceedings of 19th International Specialty Conference on Recent Research and Developments in Cold-Formed Steel Design and Construction* (pp. 61-79). St. Louis, 14-15 October.

Becque, J., & Rasmussen, K. J. R. (2009). Numerical investigation of the interaction of local and overall buckling of stainless steel I-columns. *Journal of Structural Engineering, 135*(11), 1349-1356.

Bleich, F. (1952). *Buckling strength of metal structures*. McGraw-Hill, New York.

Bradford, M. A., & Ronagh, H. R. (1997). Generalized elastic buckling of restrained I-beams by FEM. *Journal of Structural Engineering, ASCE, 123*(12), 1631-1637.

Canadian Standards Association (CSA). (1994). *Limit states design of steel structures*. CSA Standard S16.1-94. Canadian Standards Association, Rexdale, Ont.

CSA. (2000). *Canadian highway bridge design code*. CSA Standard S6-00. Canadian Standards Association, Rexdale, Ont.

Canadian Institute of Steel Construction (CISC). (1997). *Structural section tables (SST electronic database)*. Canadian Institute of Steel Construction, Willowdale, Ont.

CISC. (2000). *Handbook of steel construction* (7th ed., 2nd revised printing). Willowdale, Ont.: Canadian Institute of Steel Construction.

CISC. (1997). *Structural section tables (SST electronic database)*. Willowdale, Ont.: Canadian Institute of Steel Construction.

Chajes, A. (1993). *Principles of structural stability theory*. Prentice-Hall, Englewood Cliffs, New Jersey.

Cheung, Y. (1976). *Finite strip method in structural analysis*. Pergamon Press, Oxford.

Cheung, Y. K., & Tham, L. G. (1998). *The finite strip method*. CRC Press, Boca Raton.

Chidolue, C. A., & Aginam, C. H. (2012). Effects of shape factor on the torsional-flexural distortional behavior of thin-walled box-girder structures. *International Journal of Engineering and Advanced Technology (IJEAT)*, *1*(5), 469-479.

Chidolue, C. A., & Osadebe, N. N. (2012). Torsional-flexural behavior of thin-walled monosymmetric box-girder structures. *International Journal of Engineering Sciences and Emerging Technologies*, *2*(2), 11-19.

Davison, B., & Owens, G. W. (2012). *Steel designers' manual* (7th ed.). John Wiley & Sons, Ltd.

El Darwish, I. A., & Johnston, B. G. (1965). Torsion of structural shapes. *ASCE Journal of the Structural Division*, *91*(ST1).

Donnell, L. H. (1934). A new theory for buckling of thin cylinders under axial compression and bending. *Transactions of the ASME*, *56*, 795–806.

Ellifritt, D. S., & Lue, D.-M. (1998). Design of crane runway beam with channel cap. *Engineering Journal*, AISC, 2nd Quarter.

Euler, L. (1744). *Methodus inveniendi lineas curvas maximi minimive proprietate gaudentes*. Appendix: De curvis elasticis. Lausanne and Geneva.

Euler, L. (1757). Sur la force des colonnes. *Memoires de l'académie des sciences de Berlin 1757*, *13*, 252–282. In *Opera Omnia* (set 2, Vol. 17, 1982), 89–118.

Ezeh, J. C. (2009). Stability of axially compressed multi-cell thin-walled closed column (PhD Thesis). University of Nigeria, Nsukka.

Ezeh, J. C. (2010). Buckling behavior of axially compressed multi-cell doubly symmetric thin-walled column using Vlasov's theory. *International Journal of Engineering*, *4*(2), 179-194.

Galambos, T. V. (1963). Inelastic lateral buckling of beams. *Journal of the Structural Division, ASCE*, *89*(ST5), 217-242.

Galambos, T. V. (1968). *Structural members and frames*. Prentice-Hall Inc., Englewood Cliffs, N.J.

Hancock, G. J., & Trahair, N. S. (1978). Finite element analysis of lateral buckling of continuously restrained beam-columns. *Civil Engineering Transactions, Institution of Engineering, Australia*, *CE20*(2), 120-127.

Heins, C. P. (1975). *Bending and torsional design in structural members*. Lexington Books, Lexington, MA.

Hendy, C. R., & Murphy, C. J. (2007). *Designers' guide to EN 1993-2 Eurocode 3: Design of steel structures. Part 2 Steel bridges*. Thomas Telford.

Henry, P. G. (2015). *Lecture note*. Department of Civil and Environmental Engineering, Duke University, North Carolina, USA.

Horne, M. R. (1950). Critical loading condition of engineering structures (PhD Dissertation). Cambridge University, Cambridge, England.

Hughes, T. (2000). *The finite element method–Linear static and dynamic finite element analysis*. Prentice-Hall, Inc., Englewood Cliffs, N.J.

Ibearugbulem, O. M., Ezeh, J. C., & Ettu, L. O. (2014). *Energy method in theory of rectangular plates (Use of polynomial shape functions)* (1st ed.). LIU House of Excellence Ventures.

Ike, C. C. (2018). Energy formulation for flexural–torsional buckling of thin-walled columns with open cross-section. *Mathematical Modelling and Engineering Problems*.

Iyengar, N. G. R. (1988). *Structural stability of columns and plates* (1st ed.). Ellis Horwood, New York.

Jerath, S. (2020). *Structural stability theory and practice: Buckling of columns, beams, plates, and shells* (1st ed.). John Wiley & Sons, Incorporated. ISBN: 9781119694502.

Jerath, S., & Lee, M. (2015). Stability of cylindrical tanks under static and earthquake loading. *Journal of Civil Engineering and Architecture*, *9*(1), 72–79.

Kitipornchai, S., & Trahair, N. S. (1975). Elastic behavior of tapered monosymmetric I beams under moment gradient. *Journal of the Structural Division, ASCE*, *101*(8), 1661-1678.

Kitipornchai, S., & Trahair, N. S. (1980). Buckling properties of monosymmetric I-beams. *ASCE Journal of the Structural Division*, *106*(ST5).

Krolak, M., Kowal-Michalska, K., Mania, R. J., & Swiniarski, J. (2009). Stability and load carrying capacity of multi-cell thin-walled columns of rectangular cross-sections. *Journal of Theoretical and Applied Mechanics*, *47*(2), 456-456.

Lee, G. C. (1960). Literature survey on lateral instability and lateral bracing requirements. *Technical Report*.

Michell, A. G. M. (1899). Elastic stability of long beams under transverse forces. *Philosophical Magazine*, *48*(5th Series), 298-309.

Njoku, C. F. (2018). Dynamic analysis of rectangular thin isotropic plates using beam analogy method (Ph.D. thesis). Postgraduate School, Federal University of Technology, Owerri.

Nwachukwu, K. C., Ezeh, J. C., Thomas, B., Okafor, M., & Okodugha, D. A. (2017). Formulation of the total potential energy functional for a thin-walled box column applicable to Raleigh-Ritz method. *Researchjournali's Journal of Civil Engineering*, *3*(2).

Osadebe, N. N., & Chidolue, C. A. (2012a). Torsional-distortional response of thin-walled mono symmetric box girder. *International Journal of Engineering Research and Applications*, *2*(3), 814-821.

Osadebe, N. N., & Chidolue, C. A. (2012b). Response of double cell mono-symmetric box girder structure to torsional-distortional deformations. *International Journal of Engineering and Advanced Technology*, *1*(4), 285-292.

Osadebe, N. N., & Ezeh, J. C. (2009a). Stability of axially compressed single-cell mono-symmetric thin walled closed column. *Nigerian Journal of Technology*, *28*(2).

Osadebe, N. N., & Ezeh, J. C. (2009b). Flexural, torsional and distortional buckling of single-cell thin walled box columns. *Nigerian Journal of Technology*, *28*(2), 80-91.

Papangelis, J. P., Trahair, N. S., & Hancock, G. L. (1998). Elastic torsional-flexural buckling of structures by computer. *Computers and Structures*, *68*(1-3), 125-137.

Powell, G., & Klingner, R. (1970). Elastic lateral buckling of steel beams. *Journal of the Structural Division, ASCE*, *96*(9), 1919-1932.

Picard, A., & Beaulieu, D. (1991). Calcul des charpentes d'acier. Canadian Institute of Steel Construction, Willowdale, Ont.

Prandtl, L. (1899). Kipperscheinungen. Dissertation des Universitat Munchen. Reddy, J. N. (1993). *An Introduction to Finite Element Method* (2nd ed.). McGraw-Hill, Inc., New York.

Rozylo, P., & Debski, H. (2020). Stability and load-carrying capacity of short composite Z-profiles under eccentric compression. *Thin-Walled Structures*, *157*, 107019.

Rozylo, P., Ferdynus, M., Debski, H., & Samborski, S. (2020). Progressive failure analysis of thin walled composite structures verified experimentally. *Materials*.

Salmon, C. G., & Johnson, J. E. (1980). *Steel Structures, Design and Behavior* (2nd ed.). New York, NY: Harper & Row, Publishers.

Sallstrom, J. H. (1996). Accurate calculation of elastic buckling loads for space frames built-up of uniform beams of open thin-walled cross-section. *International Journal of Numerical Methods in Engineering*, *39*, 2319-2333.

Schardt, R. (1994). Lateral torsional and distortional buckling of channel- and hat-sections. *Journal of Constructional Steel Research*.

Seaburg, P. A., & Carter, C. J. (1997). *Torsional Analysis of Structural Steel Members*. American Institute of Steel Construction, Chicago, Ill.

Shanmugam, N. E., Richard Liew, J. Y., & Lee, S. L. (1989). Thin-walled steel box columns under biaxial loading. *Journal of Structural Engineering*, *55*(12), 742-748.

Simao, P., & Simoes da Silva, L. (2004). A numerical scheme for post-buckling analysis of thin-walled members in the context of GBT. In *Proceedings of Advances in Computational and Experimental Engineering and Science* (pp. 2079-2086). Tech Science Press.

Structural Stability Research Council (SSRC). (1998). *Guide to Stability Design Criteria for Metal Structures* (5th ed.). Edited by T. V. Galambos, Structural Stability Research Council, John Wiley & Sons, New York, N.Y.

Stelco. (1981). *Hollow Structural Sections - Sizes and Section Properties* (6th ed.). Stelco Inc., Hamilton, Ont.

St. Venant, A. J. C. B. (1855). Memoire sur la torsion des prismes. *Mem. Divers Savants*, *14*, 233-560. Timoshenko, S. P., & Gere, J. M. (1961). *Theory of Elastic Stability* (2nd ed.). McGraw-Hill, New York.

Fang, P. J., & Winter, G. (1965). *Torsional-flexural buckling of thin-walled open sections* (Report No. 158). CCFSS Library, Missouri University of Science and Technology. https://scholarsmine.mst.edu/ccfss-library/158

Timoshenko, S. P., & Gere, J. M. (1961). *Theory of elastic stability* (2nd ed.). McGraw-Hill.

Tong, G., & Lei, Z. (2003a). The transverse stresses in thin-walled beams and its effect on strength and stability. *Advances in Structural Engineering*, *6*, 159–167.

Tong, G., & Lei, Z. (2003b). An analysis of current stability theories for thin-walled members. *Advances in Structural Engineering*, *6*(4), 283–292.

Torkamani, M. A. M., & Erin, R. R. (2009). Energy equations for elastic flexural–torsional buckling analysis of plane structures. *Thin-Walled Structures*, *47*(4), 463-473.

Trahair, N. S. (1968). Elastic stability of propped cantilevers. *Civil Engineering Transactions, Institution of Engineering, Australia*, *CE10*(1), 94-100.

Trahair, N. S. (1993). *Flexural–Torsional Buckling of Structures*. CRC Press Ann Arbor.

Wagner, H. (1929). Torsion and buckling of open sections. In *25th Anniversary Publication*, Technische Hochschule, Danzig.

Wang, C. M., Wang, L., & Ang, K. K. (1994). Beam-buckling analysis via automated Rayleigh-Ritz method. *Journal of Structural Engineering, ASCE*, *120*(1), 200-211.

White, M. W. (1956). The lateral torsional buckling of yielded structural steel members. (PhD Dissertation), Lehigh University, Bethlehem, Pennsylvania.

Wittrick, W. H. (1952). Lateral instability of rectangular beams of strain hardening material under uniform bending. *Journal of Aeronautical Science*, *19*(12).

Yu, W.-W., LaBoube, R. A., & Yu, W. (2010). *Cold-Formed Steel Design* (4th ed.). John Wiley & Sons, Incorporated. ISBN: 9780470919743.